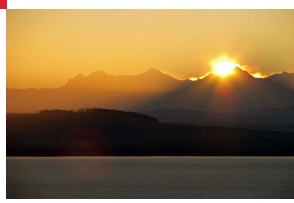

Abstract Volume
7th Swiss Geoscience Meeting

Neuchâtel, 20th – 21st November 2009

3. Mineralogy-Petrology-Geochemistry

sc | nat

Geosciences
Platform of the Swiss Academy of Sciences

chyn
Centre d'hydrogéologie

3. Mineralogy-Petrology-Geochemistry

Bernard Grobéty, Eric Reusser

Swiss Society of Mineralogy and Petrology (SSMP)

3.22 Márquez-Zavalía F., Heinrich C.A., Meier D.: Ore fluid evolution in a volcanic-hosted epithermal ore deposit: Farallón Negro, Argentina

3.23 Mattsson H., Bosshard S.: Columnar jointing and the formation of "chisel-marks" in the Hrossadalur lava flow, northern Iceland

3.24 Mattsson H., Reusser E.: Baggalútar from Hvalfjördur, SW Iceland: Volcanic spherulites or not?

3.25 Monnard H, Manzella I., Phillips J., Bonadonna C.: Convective Instabilities in Volcanic Clouds

3.26 Monsef I., Rahgoshay M., Emami M.H., Shafaii M.: Geochemical constraints on the development of a Mesozoic volcanotectonic arc and fore-arc basin in the Sanandaj-Sirjan Zone, south Iran

3.27 Monsef R., Emami M., Rashidnejad Omran N.: Transtensional basin system in Central Iranian Volcanic Belt

3.28 Moulas E., Kostopoulos D.: Metamorphic evolution of a kyanite-eclogite from Thermes, Rhodope Massif, Greece

3.29 Pistone M., Caricchi L., Burlini L., Ulmer P.: Rheological properties of crystal- and bubble-bearing silicic magmas: preliminary experimental results

3.30 Regis D., Manzotti P., Boston K., Cenki-Tok B., Robyr M., Rubatto D., Thomsen T., Engi M.: Complexities in the high pressure metamorphic history of the central Sesia Zone near Cima di Bonze (NW Italy)

3.31 Reitsma M., Schaltegger U., Spikings R., Carlotto V.: The temporal evolution of the Mitu group, south-east Peru - first U-Pb age data.

3.32 Rosa A., Sanchez-Valle C., Wang J., Saikia A.: Single-crystal elastic properties of superhydrous phase B determined by Brillouin scattering spectroscopy

3.33 Scalisi R., Costantini L., Bonadonna C., Di Muro A.: The influence of volatiles in basaltic explosive eruptions: the example of the Chaimilla eruption (3.1 Ka, Villarrica Volcano, Chile).

3.34 Semytkivska N., Ulmer P.: An experimental study in the system Fe-Mg-Ti-Cr-Si-O±Al: ilmenite solid solution as a function of pressure and temperature

3.35 Sergeev D., Dijkstra A.: Pyroxenite veins in the Jurassic Pindos Ophiolite (NW Greece): cm-scale mantle heterogeneity preserved in MORB-source peridotites

3.36 Shafaii H., Stern R., Rahgoshay M.: The Zagros Collision Zone: Petrological and geodynamical constraints on Inner and Outer Zagros Ophiolitic Belt

3.37 Skopelitis Al., Bachmann O.: The transition from cold-wet to hotter-drier rhyolites in subduction zones: the case of the Kos-Nisyros-Yali volcanic center, Aegean arc, Greece

3.38 Tercier-Waeber M.-L., Hezard T., Masson M.: Dynamics of Cd, Pb and Cu cycling in a stream under contrasting photobenthic biofilm activity and hydrological conditions.

3.39 Thomsen T., Pettke T., Allaz J., Engi M.: LAMBERN – software U-Pb, Th-Pb and Pb-Pb age dating by LA-ICP-MS analysis

3.40 Trittschack R., Grobéty B.: First insights into the dehydration of lizardite

3.41 Tsunematsu K., Bonadonna C., Falcone J.L., Chopard B.: Analytical and numerical description of tephra deposition: the example of two large explosive eruptions of Cotopaxi Volcano, Ecuador

3.42 Udry A., Müntener O.: Petrology of mafic-ultramafic complexes within the Archean Lewisian complex of NW Scotland

3.43 Vils F., Dijkstra A., Pelletier L., Ludwig T., Kalt A.: Iridium-strip heater glass pellets: Effects of fusion temperature and time on Li, Be and B content

3.44 Voegelin A., Samankassou, E., Nägler T.: Molybdenum isotopes in modern corals: investigation into their potential as redox proxy of bygone oceans

3.45 Wang J., Sanchez-Valle C., Stalder R.: Effect of minor elements (H^+ and Al^{3+}) on the elastic properties of orthopyroxenes

3.46 Wiederkehr M., Bousquet R., Masafumi S., Ziemann M., Berger A., Schmid S.: Deciphering the Alpine orogenic evolution from subduction to collisional thermal overprint: Raman spectroscopy and 40Ar/39Ar age constraints from the Valaisan Ocean (Central Alps)

3.47 Zurfluh F., Hofmann B., Gnos E., Eggenberger U., Opitz C.: Approximate terrestrial age dating of meteorites by use of handheld XRF

3.1

Apport des donnees des rayon x, de crystallographie et des inclusions fluides dans la determination de l'origine et la composition mineralogiques de la serie barytine -celestite du gisement d'Ain Allega. Tunisie septentrionale.

ABIDI Riadh *; SLIM-SHIMI Najet ** ; HATIRA Nouri *; MEJRI Zouhaier *

*: *Faculté des sciences de Bizerte, département de géologie, Jarzouna-Bizerte.7021. Tunisie.*
**: *Faculté des sciences mathématiques, physiques naturelles de Tunis. Campus Universitaire. 1060 Tunis. Tunisie.*
E.mail :abidi1riadh@yahoo.com ; najetshimi@yahoo.fr ; nouri_hatira@yahoo.fr ; mejrizouhair@yahoo.fr

Le gisement d'Ain Allega et de type « Cap-rocks » est situé sur la bordure orientale du diapir d'Ain Allega. La minéralisation est discordante par apport à la roche encaissante, elle se présente sous forme de ciment des brèches, sous forme de remplissage des fractures et des cavités de dissolution et sous forme de remplacement de la roche encaissante (Dolomie d'âge triasique). ce gisement présent une simple minéralisation composé par la galène, la saphalerite, la marcasite et la pyrite avec une gangue représenté par la barytine, la célestite, la dolomite, la calcite et le quartz. L'étude pétrographique des minéraux de la série barytine – célestite montre qu'ils possèdent plusieurs faciès en particulier microfibreux, saccharoïde, fibrolamellaire et prismatique.

L'étude radiocristallographique des minéraux de cette série barytine célestite ((Ba_X, Sr_{1-X}) SO_4) avec X [0-1]) prouve qu'on a une variété d'espèces de minéraux dont on a barytine pure (100% $BaSO_4$) abondant, célestite pur (100% $SrSO_4$) abondant, barytine srantianfère (85 to 96.5 % $BaSO_4$) minoritaire et célestite-baryfère (95% $SrSO_4$) minoritaire. Ces minéraux varie entre eux selon le degré de substitution de strontium (Sr) par le baryum (Ba) dans la celestite ($SrSO_4$) et le degré de substitution de baryum par le strontium dans la barytine ($BaSO_4$). Cette substitution est très bien visible dans les diffractogrammes au rayons X des minéraux de cette série qui est matérialisé par la variation de la position, l'intensité et la morphologie des raies 200, 011, 113, 312 de la barytine et la barytine strantianitère et les rais 410, 401 et 122 de la célestite et la célestite baryfére et aussi variation de la distance réticulaire du pic principal de la barytine de 3.44 à 3.42 pour la barytine strantianitère (fig.1).

L'étude des inclusions fluides contenues dans la célestite pur a montré que les inclusions primaire et secondaire monophasées à liquide sont les plus abondantes. Les mesures microthermométriques prouve que le fluide minéralisateur est d'origine hydrothermale et qui est caractérisé par une température d'homogénéisation élevais (180°C) et une salinité moyenne à élevais (16 % poids éq NaCl). Le rapport entre la température d'homogénéisation et la salinité (fig. 2) indique que la saumure de basin avec une certaine introduction de fluide de mélange magmatique - météorique était responsable de la minéralisation de minerai d'Ain Allega. La salinité élevée de cette solution ait résulté de la lixiviation et la dissolution des unités évaporitiques du Trias.

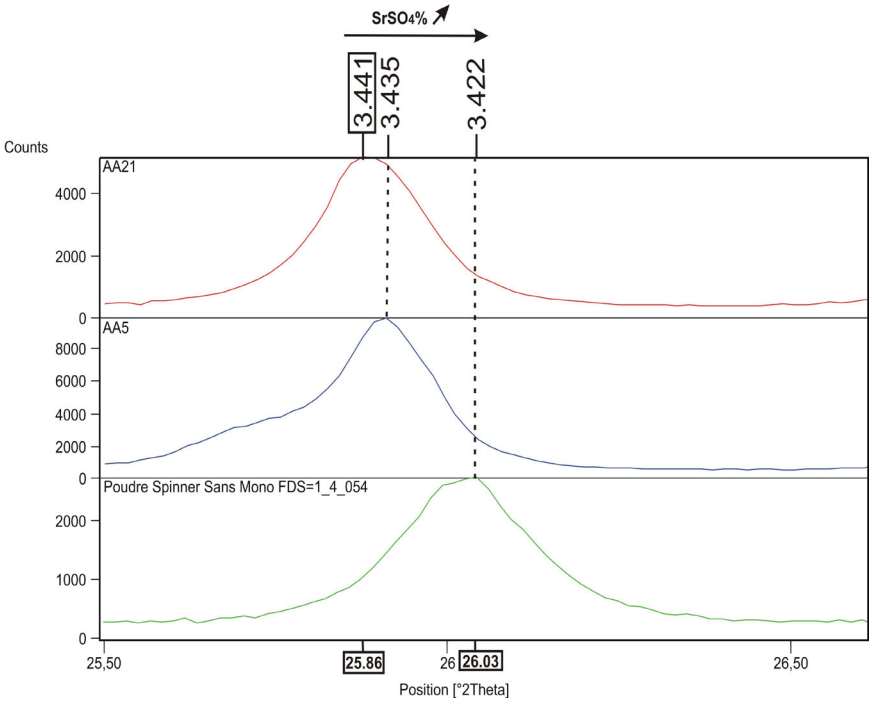

Figure. 1. Variation de la position du pic principal de la barytine en fonction du degré de substitution de Baryum par Strontium dans la barytine.

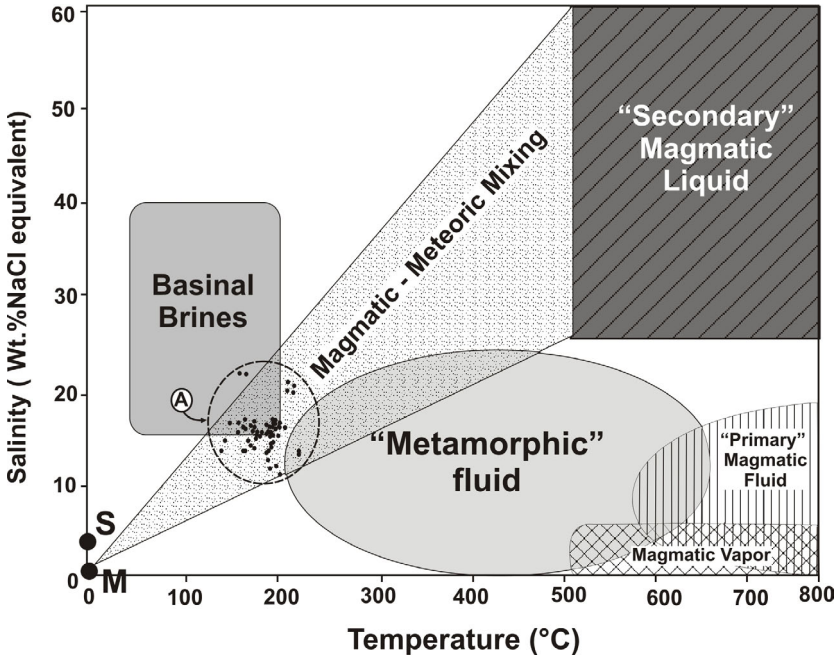

Figure.2. Diagramme de corrélation binaire température –salinité des inclusion fluides dans la célestite du gisement d'Ain Allega

3.2

Tephra Stratigraphy of the May, 2008, Chaiten Eruption, Chile

F. Alfano1, C. Bonadonna1, A. C. M. Volentik2, C. B. Connor3, S. F. L. Watt4, D. M. Pyle4, L. J. Connor3

1. Department of Mineralogy, University of Geneva, rue des Maraichers 13, CH-1205 Geneva, Switzerland.
2. Department of Geology and Geophysics, Volcanology, Geochemistry and Petrology University of Hawai'I, 1680 East-West Road, POST 614B, Honolulu, HI 96822
3. Department of Geology - SCA 528, University of South Florida, 4202 E. Fowler Ave., Tampa, FL, 33620, USA.
4. Department of Earth Sciences, University of Oxford, Parks Road, OX1 3PR, UK

Abstract. On May 2 2008 Mount Chaiten, located in the southern Chile, on the northern sector of Patagonia, after only 36 hours of precursory seismic activity, interrupted a long period of quiescence of more than 9000 years, producing his first historical eruption and causing the spontaneous evacuation of Chaiten village, located few km from the vent. The 2008 eruption of Chaiten is considered to be the largest volcanic event since the eruption of Hudson volcano (Chile) in 1991, and the first rhyolitic event since the eruption of Novarupta (Alaska) in 1912. The activity was characterized by several explosive events associated with plumes up to 20 km a.s.l. The products have been dispersed in a wide area (more than 200 km of distance from the crater), with the finest ash reaching the Atlantic coast of Argentina. Satellite images clearly show the developing of the counterclockwise rotation of the dispersal axis from SSE to NNE related to a shift in wind direction. Our field observations in the medial area (5-20 km from the vent) indicate that the May 2008 tephra deposit consists of numerous layers, most of which can be correlated with individual small explosions and subsequent fallout events. These layers vary from extremely fine-grained tephra to layers of lapilli and large blocks, composed of both juvenile and lithic material. In distal area (>200 km), the fallout deposit consists only of white to grey fine and coarse ash, eventually containing some accretionary lapilli. Although the May 2008 eruption was of moderate volume, tephra fallout had a substantial impact in terms of generation of lahars (in proximal-medial area, up to 20 km far from the vent), damage to vegetation (i.e. forests and crops) and remobilization of fine ash with effects to human and animals health. In this work we propose a reconstruction of the stratigraphy of the first events, which took place between 2nd and 8th May 2008 and a first physical characterization of the eruption. The medial stratigraphy associated with the four main explosive events could be recognized: 2nd-3rd May, 4th-5th May, 6th-7th May and 8th May, with an estimated cumulative volume of 0.118±0.057 km^3 (integration of power-law fitting) For the last event, represented by a layer composed mainly of lithic lapilli and blocks (>2 mm), an isopleth map was compiled and the associated plume height was determined. The plume is estimated to be about 19 km, when calculated considering the average of the geometric mean of the three axes of the 5 maximum clasts, and about 17 km, when calculated considering the geometric mean of the three axes of the 50th percentile clast. These values are close to the satellite observations for the event of the 8th May (i.e.about 20 km a.s.l.).

3.3

Metamorphic evolution of the Qinling Group, Qinling belt, east central China

Bader Thomas*, Franz Leander*, de Capitani Christian*, Ratschbacher Lothar**, Hacker Bradley R.***, Weise Carsten**, Wiesinger Maria**, Popp Michael**

*Mineralogisch-Petrographisches Institut, Universität Basel, CH-4056 Basel
(thomas.bader@unibas.ch)
**Institut für Geologie, Technische Universität Bergakademie Freiberg, D-09599 Freiberg
*** Geological Sciences, University of California, Santa Barbara, CA-93106

The Qinling Group, part of the Upper Proterozoic-Triassic Qinling belt, mainly comprises felsic gneisses, amphibolites and marbles. It can be subdivided into two parts. The northern margin experienced a Cambrian ultrahigh-pressure metamorphism as evident by the occurrence of diamond inclusions in metamorphic zircon (Yang et al., 2003). The central-southern part was affected by migmatisation within a Devonian magmatic arc caused by a northward trending subduction zone facing the Qinling orogen (Ratschbacher et al., 2003, for a review). Few data on the metamorphic evolution of the southern part of the Qinling Group were published by You et al. (1993) while such data are lacking for the northern margin. In the current study, we present new petrologic data for both parts derived by means of equilibrium phase calculations and conventional geothermobarometry combined with $^{40}Ar/^{39}Ar$ and Th/Pb geochronology.

Eclogites from the Northern margin of the Qinling Group are fine to medium-grained, weakly foliated rocks that occur as lenses with diameters up to 2m mantled by phengite gneisses. Texturally, our samples give indications for the UHP event by numerous radial cracks around quartz inclusions in garnet pointing to former coesite. The assemblage of the pressure peak comprises garnet (core) – omphacite – coesite – phengite – rutile. However, modelling using the DOMINO program and the application of conventional geothermobarometers yielded quartz-eclogite facies conditions of ~ 600 °C at 1.8-2.2 GPa representing an early exhumation stage. The exhumation history of the eclogitic rocks is further constrained by the late amphibolite facies mineral assemblage garnet (rim) – amphibole – plagioclase – quartz – ilmenite pointing to ~650 °C at 1.0-1.4 GPa. This was verified by conventional thermobarometry on garnet amphibolite 75221 C and garnet gneiss 75214D from the same unit pointing to 630-660°C at 1.0 GPa (fig. 1, left).

The central and southern parts of the Qinling Group reveal high-grade metamorphic PT conditions as evident by migmatisation of felsic gneisses. Peak metamorphic assemblages in metapelitic gneisses comprise garnet – plagioclase – K feldspar – quartz – sillimanite – ilmenite and garnet – hornblende – plagioclase – quartz – ilmenite in metabasites. PT estimates using the DOMINO program and conventional geothermobarometry point to 600-730 °C at 0.3-0.7 GPa (fig. 1, right). The lower PT conditions are interpreted to indicate a retrograde development of the metamorphism. No indication of eclogite facies metamorphism was found in the gneisses and amphibolites. However, the finding of a small body of strongly overprinted spinel peridotite in the southern part of this profile, which had re-equilibrated to 630-670 °C (i.e. identical temperatures to the surrounding gneisses and amphibolites), points to a probable early HP event.

$^{40}Ar/^{39}Ar$ dating of phengites from the northern margin of the Qinling Group yields 470±1 Ma. Significantly younger ages were obtained by dating metamorphic monazite (Th/Pb, 340-395 Ma), hornblende ($^{40}Ar/^{39}Ar$, 373-395 Ma) and biotite ($^{40}Ar/^{39}Ar$, 330-390 Ma) from the central and southern Qinling Group.

These findings prove that the exhumation of the UHP metamorphics took place in Early- to Mid-Ordovician. The rocks of the central-southern Qinling Group underwent a Devonian ultra metamorphism in the middle crust within a magmatic arc setting with high heat flow. Further investigations will show, how both subunits had been juxtaposed.

REFERENCES

Ratschbacher, L., Hacker, B.R., Calvert, A., Webb, L.E., Grimmer, J.C., McWilliams, M., Ireland, T., Dong, S. & Hu, J. 2003: Tectonics of the Qinling Belt (Central China): Tectonostratigraphy, geochronology, and deformation history. Tectonophysics 366, 1-53.

Yang, J., Xu, Z., Dobrzhinetskaya, L. F., Green II, H. W., Pei, X., Shi, R., Wu, C., Wooden, J. L., Zhang, J., Wan, Y., Li, H., 2003: Discovery of metamorphic diamonds in central China: an indication of a > 4000-km-long zone of deep subduction resulting from multiple continental collisions. Terra Nova, 15, 370-379.

You, Z., Han, Y., Suo, S., Chen, N. & Zhong, Z., 1993: Metamorphic history and tectonic evolution of the Qinling Complex, eastern Qinling Mountains, China. Journal of metamorphic Geology, 11, 549-560.

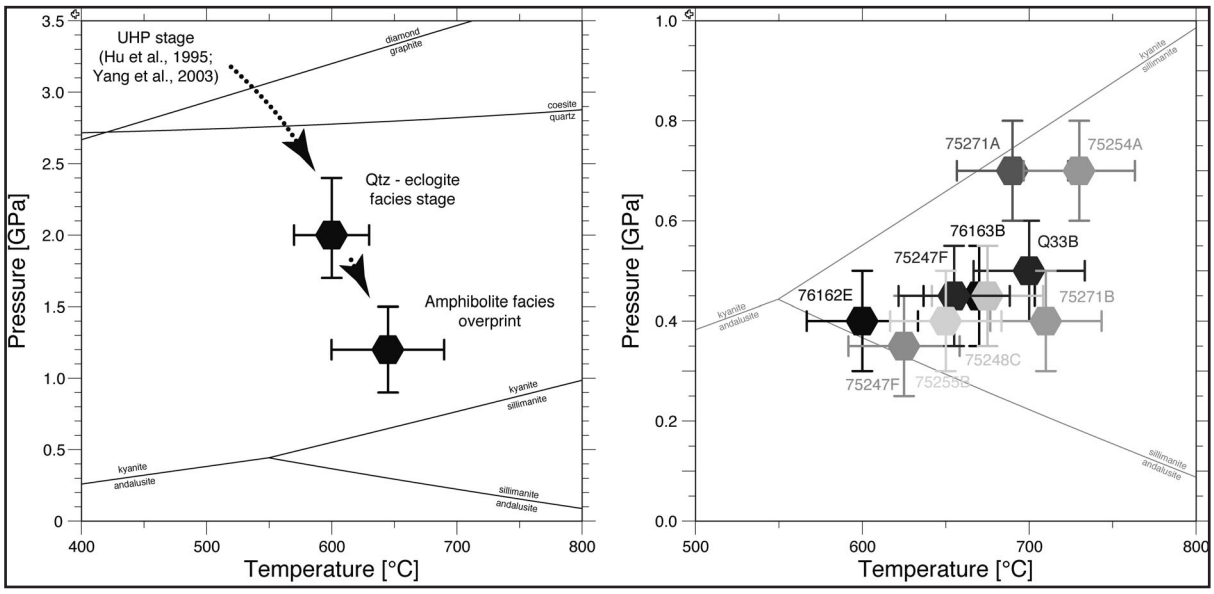

Figure 1: left: Metamorphic development of the northern margin of the Qinling Group. Right: PT estimates of the central-southern Qinling Group.

3.4

Stable isotopes in precipitation as proxies for the Neogene topographic and climatic evolution of the Alps

Bauer Kerstin*,**, Vennemann Torsten*, Mulch Andreas**

*Institut de Minéralogie et Géochimie, Anthropole, Université de Lausanne, CH-1015 Lausanne, Switzerland (Kerstin.Bauer@unil.ch)
** Institut für Geologie, Leibniz Universität Hannover, Callinstr. 30, 30167 Hannover, Germany

The paleoelevation of a mountain belt is an important parameter to understand its evolution and sets constraints on uplift and erosion rates and also on the paleoclimate. A quantitative tool to determine this is the altitude effect on the stable isotope composition of precipitation, since the $\delta^{18}O$ and δD values in precipitation decrease with elevation.

Precipitation of the past can be preserved in surface-formed hydrous silicates and also, after infiltration via faults and shear zones, in metamorphic minerals which interacted with meteoric water and/or trapped this water as fluid inclusions.

This study aims to reconstruct the changes in isotopic composition of precipitation and thus palaeoelevation of the European Alps during the Miocene. Therefore, isotopic compositions of minerals derived from surface alteration and/or fault gauges of different localities in the Alps will be studied.

To obtain a correction for the climatic conditions which can also change the $^{18}O/^{16}O$ and D/H ratios, low elevation material from the Alpine foreland covering the same time period will also be analyzed. Clay minerals from the Molasse basin appear to be promising material and paleoclimate information derived for sea level conditions from several of these layers already exist from studies of marine fossils.

Additionally, samples will be analyzed from present soil horizons to further examine the local dependences of isotopic variations with elevation and the uptake of the isotopic composition from rainwater into the minerals formed.

REFERENCES

Janz, H. & Vennemann, T. W., 2005: Isotopic composition (O, C, Sr and Nd) and trace element ratios (Sr/Ca, Mg/Ca) of Miocene marine and brackish ostracods from North Alpine foreland deposits (Germany and Austria) as indicators for paleoclimate. Palaeogeography, Palaeoclimatology, Palaeoecology 225 (2005), 216-247.

Kocsis, L., Vennemann, T. W., Hegner, E., Fontignie, D., & Tütken, T., 2009: Constraints on Miocene oceanography and climate in the Western and Central Paratethys: O-, Sr-, and Nd-isotope compositions of marine fish and mammal remains. Palaeogeography, Palaeoclimatology, Palaeoecology 271 (2009), 117-129.

Mulch, A., Teyssier, C., Cosca, M. A., Vanderhaeghe, O., & Vennemann, T. W., 2004: Reconstructing paleoelevation in eroded orogens. Geology 32, 6 (2004), 525-528.

Mulch, A. & Chamberlain C. P., 2007: Stable Isotope Paleoaltimetry in Orogenic Belts – The Silicate Record in Surface and Crustal Geological Archives. Reviews in Mineralogy & Geochemistry 66 (2007), 89-118.

3.5

Mineralogy, Fluid inclusions and sulphur isotope investigation of the Pb-Zn-Ba-(Sr) deposits at Oued Jebs-Kef Lasfar, North Tunisia

Jaloul BEJAOUI *, Ahmed SELLAMI ** and S. A. SKAGGS ***

* *Centre National des Sciences et Technologies Nucléaires, Tunisie, bjaoui_geo@yahoo.fr*
** *Office National des Mines, Tunisie*
*** *Department of Geology, University of Georgia, 210 Field St, Athens, GA 30602, USA*

The Oued Jebs-Kef Lasfar Pb-Ba-Zn-(Sr) deposit is located in northern Tunisia, 60 Km from Tunis (Fig.1). Sulfides mineralization is mainly associated with Cenomanian-Turonian inter-layered limestone and marls of the Cretaceous, which replace carbonate, cemented breccias and cavities (Fig.2).

The geology of the area is dominated by massive limestone and marly limestone units of Cretaceous age, which are extensively folded. The ore deposit consists of a system of mineralized veins and breccias, extending over an area of 15 km^2. The ore-hosting limestone layers are characterized by a strong kaolinite enrichment, in amounts directly related to the proportion of the ore minerals.

The mineralization lies mainly within the organic-rich black shale succession of the Bahloul Formation (Cenomanian-Turonian) and to a lesser extent along the transition zone between Triassic and Cretaceous), where zebra-textured celestite layers also occur (Fig. 3). The celestite-calcite rhythmites, whose structure is caused by grain size variation, occur mainly around the rising salt diapirs.

Kaolinite is associated with hydrothermal mineralization and occurs in the paragenesis of the sulfides in breccias (Fig.3).

The mineralogical characteristics of kaolinite were determined by X-ray powder diffraction and they are 7,15A° (d001) and 3,57A°(d002) and is attenuated after heating. Treatment with ethyl-glycol had no effect.

Fluid inclusions were investigated in hydrothermal barite associated with sphalerite and galena. All the observed fluid inclusions are two-phase liquid and vapor inclusions, but the aqueous fluid inclusions in barite which could be analysed, range in size from 20 to 100 μm.

Primary inclusions exhibit homogenization temperature (Th) mean values ranging from 110°C to 140°C, with salinities of 14 to 18 wt. % NaCl equiv. The microthermometric data are in agreement with those measured in the Jebel Ajered Pb-Zn-Ba ore deposit (Bejaoui et al., 2008).

Microthermometric data of fluid inclusions reveal the involvement of basinal brines in mineralization of Oued Jebs. $\delta^{34}S$ values in sphalerite and galena at Oued Jebs-Kef Lasfar range from 0.7‰ to 5.3‰. These positive values suggest an origin from evaporite sulfates, followed by thermochemical reduction (Claypool et al., 1980).

The present fluid inclusions study demonstrates the involvement of basinal brines in mineralization of Oued Jebs-Kef Lasfar.

Key words: basinal brines - Oued Jebs-Kef Lasfar - Fluid inclusions- Pb-Zn-Ba-(Sr).

Acknowledgments
We are grateful to Pr. Maria BONI for helpful comments and suggestions.

REFERENCES

Bejaoui J., Bouhlel S., Cardellach E., and Piqué À. (2008) - Mineralogy and fluid inclusion study of carbonate hosted Pb-Zn-Ba-(Cu) deposits in Jebel Ajered, Central Tunisia. 6 Swiss Geoscience Meeting (SGM) 2008, 173-175.

Claypool G.E, Holseer W.H., Kaplan I.R., Sakai H., and Zak I. (1980) - The age curve of sulphur and oxygen isotopes in marine sulphate and their mutual interpretation. Chem. Geol., 28, 163-187.

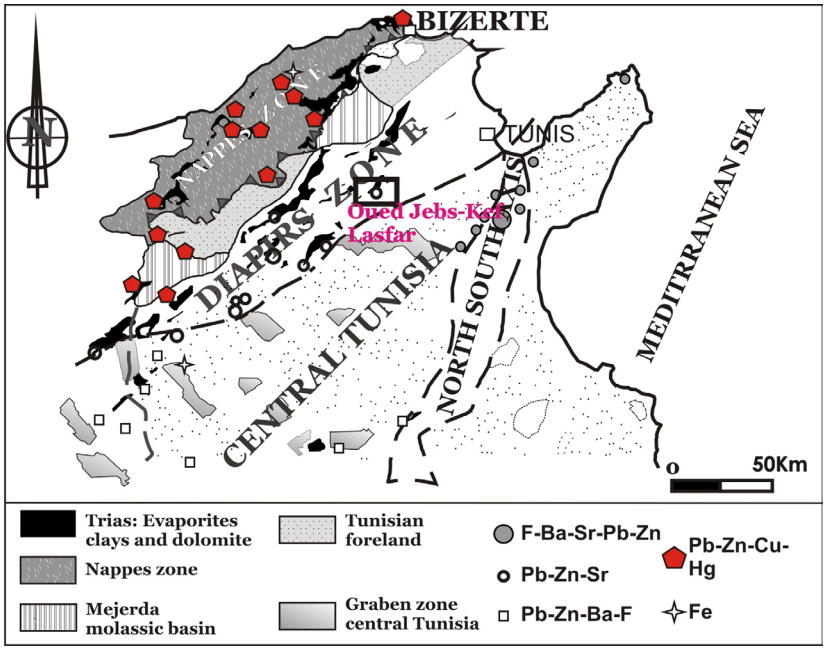

Fig 1. Location of the Oued Jebs ore deposit within the diapirs zone in Tunisian structural map.

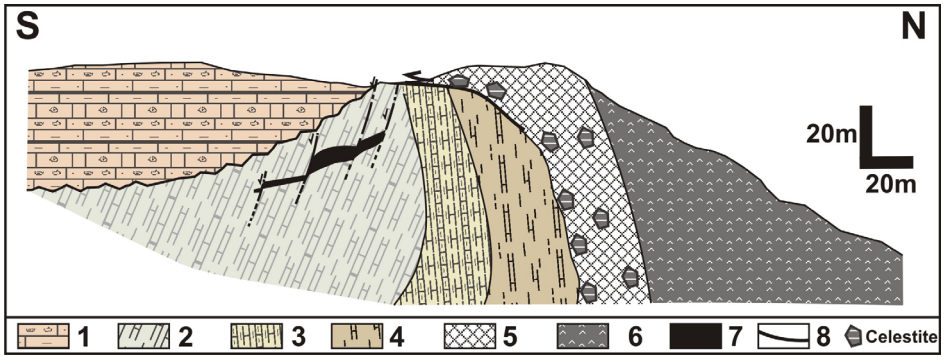

Fig 2. Cross section of Oued Jebs Pb-Zn-Ba-(Sr) ore deposits. : 1 Eocene: bioclastic limestone and marls, 2 Cenomanian-Turonian: marly limestone, 3 Albian: marl and limestone, 4 Aptian: carbonate series within silty clay layers. 5 transition zone: marls and dolomite-rich "zebra" celestite, 6 Trias: evaporites, 7: Pb-Zn-Ba-(Sr) orebodies, 8 faults.

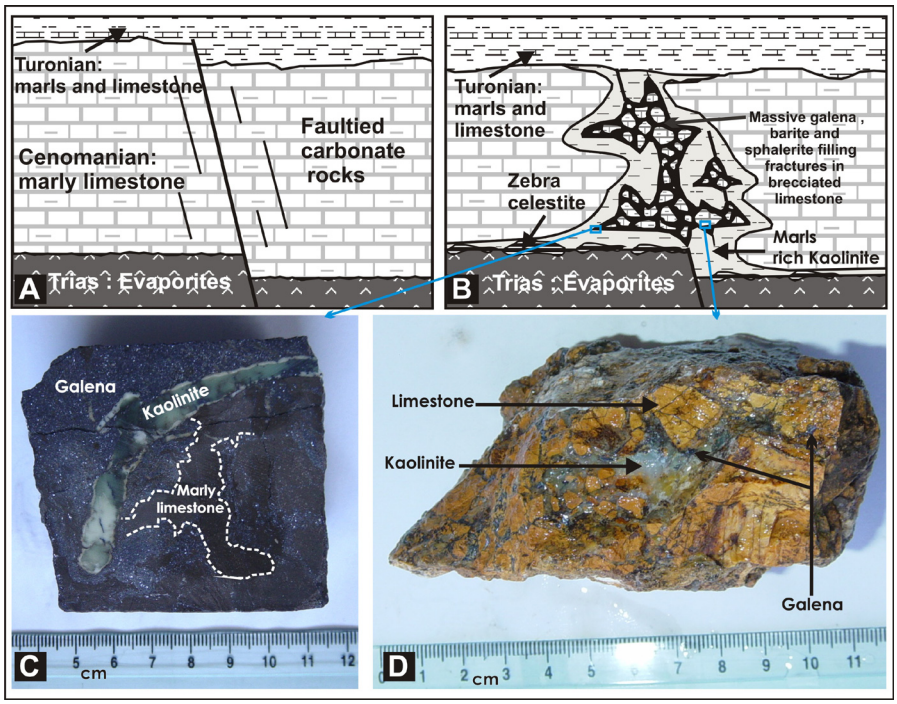

Fig 3. A Cenomanian limestone affected by fault and fractures, B Mosaic breccias cemented by sulfides mineralization, C Marls rich in kaolinite mineralized with massive galena, D Mosaic breccias cemented with kaolinite and disseminated galena.

3.6

Geology and geochronology of the Ilo batholith of southern coastal Peru

Boekhout Flora*, Thierry Sempere**, Richard Spikings*, Urs Schaltegger*

*Earth and Environmental Sciences, Rue de Maraîchers 13, CH-1205 Genève
**IRD et LMTG, 14 Avenue Edouard Belin, 31400 Toulouse, France

In Southern coastal Peru the so-called Ilo batholith is emplaced in the 'Chocolate' formation, of Early to Middle Jurassic age, that comprises more than 1000 m of basaltic and andesitic flows, agglomerates and breccias. Previous workers have correlated the dioritic to granodioritic rocks of this intrusion with the 'Coastal Batholith' of Cretaceous to Paleogene age. However, K-Ar and Ar-Ar geochronology of plutonic rocks near the city of Ilo point to Early Jurassic ages (Clark et al. 1999, Sánchez 1983a). This part of the plutonic assemblage was thus emplaced prior to the initiation of 'Coastal batholith' emplacement.
Mafic and felsic granitoid magmas are intimately associated, as reflected by the emplacement of mixed diorite-granodiorite units. Also, mafic and felsic magma mingling north of Ilo have been observed, e.g. globular enclaves of diorite in granodiorite, elongated inclusions, both basaltic and composite (basaltic/dacitic) synplutonic dikes: thus no simple mafic to felsic intrusive sequence prevailed during batholith construction.
Our aim is to describe and interpret the history of the Ilo batholith and to discuss how the magmatic history of this batholith fits into the framework of magma genesis and modes of emplacement along the active Andean margin. This first occurence of large volumes of plutonic rocks may well represent the first stages of Andean subduction (Oliveros et al. 2006).
A combination of field observations, zircon U-Pb (LA-ICP-MS and CA-ID-TIMS) data, and element geochemistry of the batholith will be used to distinguish between different magmatic pulses and their duration. Additional Sr, Nd, Pb, Hf isotope studies will be carried out, specifying the magmatic source of the different pulses of plutonic activity.

Eastward tilting of 20-30° has exposed a complete cross-section of the batholith in map view with an north-northeastward paleo-up direction, revealing that the Ilo batholith has a tabular shape: We are therefore able to study the contact with the Chocolate formation above and below the batholith, including a sampling campaign along several cross sections through the batholith for dating and geochemical analyses.
In addition to samples from the batholith itself, clastic sedimentary rocks above and below the batholith have been sampled in order to determine their maximum depositional age by dating detrital zircons using LA-ICP-MS. In this case the same or very similar detrital zircon populations should be found in both locations (below and above the tabular plutonic body), as they were originally juxtaposed.

Preliminary data of 3 samples dated by U-Pb TIMS show a pulse of magmatism at ~164 Ma with an epsilon Hf ranging from +4 to +6.9 indicating a depleted mantle source typical of continental margin settings. The geochemical data suggest a calc-alkaline magma source.
McBride et al (1983) postulated two intrusive pulses on the basis of six conventional K- Ar dates on four granitoid samples in the Ilo area of Late Jurassic (ca. 151 – 159 Ma) and mid- Cretaceous (96 – 111 Ma). Sánchez (1983a) obtained similar Albian K-Ar dates for several granodioritic samples northeast of Ilo but also found Early to Middle Jurassic dates (196-182 Ma) for two dioritic rocks from the coastal zone.
Our preliminary data might indicate another magmatic pulse, or show a longer duration of one of the previously decribed pulses.

REFERENCES

Clark Alan H, Farrar Edward, Kontak Daniel J., Langridge Robert J. 1999: Geological an Geochronological Constraints on the Metallogenic Evolution of the Andes of Southeastern Peru, Economic Geology, 85, 1520-1583.

Oliveros Veronica, Féraud Gilbert, Aguirre Luis, Fronari Michel, Morata Diego 2006 : The Early Andean Magmatic Province (EAMP) : 40Ar/39Ar dating on Mesozoic volcanic and plutonic rocks from the Coastal Cordillera, northern Chile, Journal of Voclanology and Geothermal Research, 157, 311-330.

McBride, S.L., Robertson, R.C.R., Clark, A.H., and Farrar, E. 1983: Magmatism and metallogenetic episodes in the northern tin belt 'Cordillera Real' Bolivia, Geol. Rundschau, 72, 685 – 713.

Sánchez, A. W., 1983: Edades K-Ar en rocas intrusivas del area de Ilo, Dpto. de Moquegua, Geol. Soc. Peru Bol, 71, 183 – 192.

3.7

Melt inclusions from Volcan Llaima (38.7°S, Andean Southern Volcanic Zone, Chile): Insights into shallow magma storage and crystallization

Bouvet de Maisonneuve Caroline*, Dungan Michael*, Bachmann Olivier** & Burgisser Alain***

* *Département de Minéralogie, Rue des Maraîchers 13, CH-1205 Genève (caroline.bouvet@unige.ch, Michael.Dungan@unige.ch)*
** *University of Washington, Earth and Space Sciences, Seattle, WA 98195-1310 (bachmano@u.washington.edu)*
*** *Institut des Sciences de la Terre d'Orléans - CNRS, Fr-45071 Orléans (burgisse@cnrs-orleans.fr)*

Olivine-hosted melt inclusions in scoria from four large historic eruptions of Llaima are used to elucidate processes of magma differentiation, recharge, mixing, and eruption triggering. These deposits were produced as violent Strombolian eruptions of crystal-rich mafic magma (<6 wt% MgO; 25-45% plag+oliv±cpx) associated with voluminous lava flows. Major element melt inclusion compositions are highly diverse in single samples (50-58 wt% SiO_2; 6-3 wt% MgO). These overlap with the whole-rock data trend defined by the entire volcano up to 53-55% SiO_2, but more evolved compositions form a divergent, linear trend up to >2 wt% TiO_2 with Al_2O_3 as low as 12.5 wt% at 57-58 wt% SiO_2, compared to 1.2-1.4 wt% TiO_2 and 16-17 wt% Al_2O_3 at 58 wt% SiO_2 in most Llaima andesitic magmas. The evolved extension of the melt inclusion trend is inferred to be the product of shallow evolution of interstitial melt during the formation of crystal mush as a consequence of degassing and decompression crystallization following magma stagnation. The suppression of FeTi-oxide stability and the dominance of plagioclase crystallization are consistent with low-P dry conditions. These observations are in accord with relatively low H_2O (dominantly 1-3.5 wt%) and CO_2 (dominantly 0-300 ppm) contents in melt inclusions (SIMS-ASU), which yield saturation pressures of ~300-500 bars (<2 km). H_2O and CO_2 contents do not correlate with major element melt composition, and melt inclusion fluid-saturation pressures do not correlate systematically with fractionation indices such as K_2O or Mg#. Corollaries to these observations are that degassed matrix glasses attached to many of these olivines are commonly less evolved than corresponding melt inclusions (generally in equilibrium with host olivines), olivine core compositions in single samples are diverse (Fo_{69-83}), and many of these olivines are reversely zoned to rims of Fo_{77-79}. The absence of correlated degassing and magma evolution trends in historic Llaima magmas suggests that they are stored as multiple bodies created by a higher frequency of magma replenishment in comparison to the frequency of large eruptions. This temporal-spatial disconnection leads to isolated evolution and degassing of discrete magma batches, followed by assembly just prior to eruption. Injection of relatively hot and mafic gas-rich magma is probably the triggering mechanism, in accord with and higher Olivine-Melt temperatures recorded by relatively primitive matrix glasses.

3.8

Unzipping of crystal mush as a rapid mechanism to remobilize and homogenize magma bodies

Burgisser Alain*, Bergantz George**

* *ISTO, CNRS - University of Orléans, 1a rue de la Férollerie, 45071 Orléans cedex 2, France (burgisse@cnrs-orleans.fr)*
** *Dept. of Earth and Space Sciences, University of Washington, Box 351310, Seattle, WA 98195-1310 USA*

The largest products of magmatic activity on Earth, the great bodies of granite and their corresponding large eruptions, have a dual nature: homogeneity at the large scale and spatial and temporal heterogeneity at the small scale. This duality calls for a mechanism that *1)* removes selectively the large-scale heterogeneities associated with the incremental assembly of these magmatic systems and *2)* occurs rapidly despite crystal-rich, viscous conditions seemingly resistant to mixing.

We present a simple dynamic template can unify a wide range of seemingly contradictory observations from both large plutonic bodies and volcanic systems by a mechanism of rapid remobilization ("unzipping") of highly viscous crystal-rich mushes. We demonstrate that this remobilization can lead to rapid overturn and produce the observed juxtaposition of magmatic materials with very disparate ages and complex chemical zoning. What is novel about our model is the recognition that the process has two stages. Initially a stiff mushy magma is reheated from below producing a reduction in crystallinity that leads to the growth of a subjacent buoyant mobile layer. A second stage occurs when the thickening mobile layer

becomes sufficiently buoyant to penetrate the overlying viscous mushy magma and produce rapid overturn of the entire system. This process exports homogenized material from the lower mobile layer to the top of the system, and leads to partial overturn within the viscous mush itself as an additional mechanism of mixing.

The agreement between calculated and observed unzipping rates for historical eruptions at Pinatubo and at Montserrat demonstrates both the general applicability of the model and the ability of unzipping to rapidly produce large amounts of mobile magma available for eruption. This mechanism furthers our understanding of the bifurcation between crust building by formation of periodically homogenized plutons and ignimbrite formation by large eruptions.

3.9

Behaviour of allanite during mylonitisation and implications for U-Th-Pb dating: case study at the Mt Mucrone, Italy

Cenki-Tok Bénédicte* , Oliot Emilien**, Thomsen Tonny B.*, Berger Alfons***, Spandler Carl****, Rubatto Daniela*****, Robyr Martin*, Manzotti Paola*, Regis Daniele*, Engi Martin* and Goncalves Philippe**

Uni. Bern, IfG, Baltzerstr. 1+3, 3012 CH-Bern (cenkitok@geo.unibe.ch)
**Uni Franche-Comté, UMR6249, 16 rte de Gray, F-25030 Besançon*
***Uni Copenhagen, Institute for Geography and Geology, Øster Voldgade 10, DK-1350 Copenhagen*
****James Cook University, 101 Angus Smith Dr, QLD 4811 Townsville, Australia*
*****Australian National University, 0200 Canberra, Australia*

Allanite occurs in meta-granodiorite showing different amounts of strain, from undeformed (a) to mylonitic (f). This body intruded the polycyclic Sesia basement at Permian times and underwent HP metamorphism and ductile deformation during the Alpine convergence. We study the effects of deformation on allanite U-Th-Pb apparent ages.
In the mylonitic rock allanite forms mm-size angular grains in a strongly recrystallised matrix and shows exclusively Permian ages, eventhough the grains are intimately linked to Alpine deformation and metamorphism. These grains occur in mm-sized lenses around which the mylonitic foliation flows. In addition to allanite, these lenses are composed of randomly oriented phengite and Ca-rich garnet (up to 30wt%). During mylonitisation these allanite grains were mechanically shielded by a robust mineral (epidote) that subsequently broke down to garnet and phengite.
The undeformed rock gives insight into allanite forming reaction. Relics of Permian magmatic monazite are found exclusively in the undeformed samples where the magmatic textures and minerals are largely preserved. Coronas of allanite, thorite and apatite surround monazite relics indicating the reaction: monazite + plagioclase + fluid —> allanite + apatite + thorite. These textures are located at the contact where magmatic biotite and plagioclase breakdown to form the HP assemblage phengite and garnet.
Alpine allanite is found in the undeformed rock. It is much smaller (ca. 200 μm), present fragmented textures with satellite neocrystals, is rich in Sr (up to 2wt%) and has a positive Eu anomaly. In medium strain rocks small (< 20 μm) Sr-rich rims around Permian allanite can be found. This indicates that Alpine allanite crystalisation is clearly associated to plagioclase breakdown (plagioclase + H2O —> jadeite + zoisite + quartz) and must have been triggered by local fluid present conditions.
The interpretation of these complex textures, microstructures and ages needs superposition of at least two events. At Permian times, mm-sized allanite rimed by epidote most probably formed in late magmatic fractures associated to fluid circulation. At Alpine times, these fractures play the role of precursor heterogeneities where ductile deformation is localized. Allanite in the mylonite is mechanically and chemically shielded during the Alpine event.
Allanite is a robust chronometer. However in case of superposition of deformation events, its Pb isotope composition may not record all the events seen by the rock. Reworking of old structures during the Alpine orogeny has to be taken into account when interpreting ages on allanite in deformed rocks. A deeper look into textures and structures – that can be misleading at a first glance – is necessary to understand the significance of U-Th-Pb in situ ages in polycyclic rocks.

3.10

Rapid transition to long-lived deep crustal magmatic maturation and the formation of giant porphyry-related mineralization (Yanacocha, Peru)

Chiaradia Massimo*, Merino Daniel*, Spikings Richard*

*Département de Minéralogie, Rue des Maraîchers 13, 1205-Genève (Massimo.Chiaradia@unige.ch)

An expanding amount of literature over the previous decade reports the occurrence of magmatic rocks with geochemical features of adakites (or adakite-like; i.e., high Sr/Y, low Yb) in association with major porphyry Cu-Au and porphyry-related epithermal deposits, and a twofold scientific debate has developed about this question: on one hand the genesis of adakite-like rock is controversial; on the other the meaning itself of the association of porphyry-type deposits with adakite-like rocks is debated.

Rocks with adakite-like features are considered to be the result, among others, of slab melting and slab melt-mantle wedge interactions (e.g., Defant and Drummond, 1990), of mafic lower crustal melting (e.g., Atherton and Petford, 1993), or of high-pressure fractional crystallization accompanied or not by the assimilation and melting of lower crust (e.g., Chiaradia et al., 2009). Discrimination between these processes is not straightforward, which has led to controversy on the origin of rocks with adakite-like signatures in many Phanerozoic arc systems. The debated origin of these rocks has propagated into contrasting models explaining the mechanisms of the association between adakite-like rocks and porphyry-type deposits in various Phanerozoic arc environments and post-collisional zones (e.g., review of Richards and Kerrich, 2007). Any hypothesis accounting for the relationships between adakite-like rocks and porphyry-type deposits should be based on a thorough petrogenetic study that is tightly coupled with the temporal evolution of magmatic rocks and their relationships with mineralization.

Here we report geochronologic, geochemical and isotopic data from adakite-like porphyritic rocks associated with the giant high-sulfidation system of Yanacocha, northern Peru, which is the world's largest gold deposit of this type. Mineralization is associated with porphyritic intrusions distributed along a ~8 km long NE-trending magmatic structural corridor. Eight of these intrusions investigated in this study range in age from 12.4 to 8.4 Ma and show systematic chemical and isotopic changes through time. In particular, rocks become systematically more felsic (andesite to rhyodacite), adakite-like and isotopically crust-contaminated through time, with a rapid transition from non adakitic to strongly adakite-like signatures occurring at about 12 Ma and within a time interval of <0.5 Ma.

Based on petrography, mineral and rock chemistry and isotopic compositions the Yanacocha intrusive magmas are interpreted to be the result of recharge assimilation fractional crystallization (RAFC) processes occurring at different crustal levels, involving amphibole-clinopyroxene-garnet fractionation at deeper levels, leading to more or less strong adakite-like signatures, and plagioclase-amphibole fractionation at shallower levels. Systematic geochemical and isotopic changes through time, coupled with plagioclase zoning and amphibole geobarometry suggest that the evolution of the magmatic system occurred through interaction of andesitic melts with an increasing length of the crustal column and shifted progressively through time towards shallower crustal levels as indicated by a decrease in adakitic indices between 11-8.4 Ma (although the rocks remained strongly adakite-like throughout) and by overall decreasing minimal pressures of amphibole crystallization.

This evolution was possibly the result of a steadily increasing compression associated with the Quechua II orogenic phase (12-10 Ma) that, by progressively slowing down magma ascent, forced magmas to evolve at a series of intermediate level chambers between the lower and upper crust. Increased compression during the Quechua II orogenic phase might have been related to the onset of subduction of the buoyant Inca oceanic plateau, estimated to occur at ~12 Ma (Gutscher et al., 1999), i.e., the same time of the onset of the rapid transition from "normal" to adakite-like signatures.

The giant Yanacocha ore system developed in coincidence with the ensuing ~3.6 My-long intrusion of adakite-like magmas formed by the above processes into a small upper crustal volume (corresponding to a surface area of ~5 km*5 km). This suggests that large-scale geodynamic processes leading to prolonged magmatic evolution at deep crustal levels might be a first-order control on the formation of giant porphyry-type systems, as is also indicated by similar magmatic evolutions in other porphyry-systems worldwide. How this occurs in detail (e.g., generation of volatile- and metal-rich oxidized magmas through high-pressure fractionation, recycling of sulfide-rich cumulates in the lower crust, focussed and long-lived magmatic input into a small upper crustal volume) requires additional investigation.

REFERENCES
Atherton, M.P., & Petford, N. 1993: Generation of sodium-rich magmas from newly underplated basaltic crust. Nature, 362, 144-146.
Chiaradia, M., Müntener, O., Beate, B., & Fontignie, D. 2009: Adakite-like volcanism of Ecuador: lower crust magmatic evolution and recycling. Contributions to Mineralogy and Petrology, in press, DOI 10.1007/s00410-009-0397-2.
Defant, M.J., & Drummond, M.S. 1990: Derivation of some modern arc magmas by melting of young subducted lithosphere. Nature, 347, 662-665.
Gutscher, M.-A., Olivet, J.-L., Aslanian, D., Maury, R., & Eissen, J.-P. 1999: The "lost Inca Plateau": Cause of flat subduction beneath Peru?. Earth and Planetary Science Letters, 171, 335-341.
Richards, J.P., & Kerrich, R. 2007: Adakite-like rocks: their diverse origins and questionable role in metallogenesis. Economic Geology, 102, 537-576.

3.11

Complex evolution of a highly explosive basaltic-andesite eruption of Villarrica volcano, Chile: the Chaimilla deposit

Costantini Licia*, Pioli Laura*, Longchamp Celine**, Bonadonna Costanza* & Clavero Jorge***

*Département de Minéralogie, Rue de Maraîchers 13, CH-1205 Genève (licia.costantini@unige.ch)
**Institute of Geomatics and Risk Analysis, Amphipôle - CH-1015 Lausanne
***Servicio Nacional de Geologia y Mineria (Sernageomin), Chile

Villarrica is a 2847-m-high basaltic-andesitic stratovolcano located in the southern Chilean Andes. It is one of the most active volcanoes in South America and it has been active for 600 ka producing about 60 eruptions in the last 450 years.
Although its historical eruptive activity has been mainly effusive and weakly explosive, with more than 30 known eruptions in the last century, Villarrica volcano also had large postglacial explosive behaviour, which produced pyroclastic density currents and tephra fallout from both the central vent and flank parasitic pyroclastic cones (Clavero and Moreno 2004). The two known largest-volume eruptions are the Licán and Pucón ignimbrites (13.8 and 3.6 ka respectively), which produced widespread pyroclastic density currents and are likely associated to caldera formation. The best-preserved and widely dispersed pyroclastic fallout is the Chaimilla deposit, which was erupted after the caldera-forming Pucón ignimbrite (~3.1 ka). After the last large eruption (1984-85), the Villarrica activity has been characterized by continuous degassing and sporadic bubble bursts (Witter et al., 2004; Gurioli et al., 2008).

We present the stratigraphy of Chaimilla deposit combined with the grain size, componentry, density, vesicularity and groundmass textures of juvenile products from selected fallout beds. These data are used to estimate the erupted volume and to constrain the eruption dynamics and evolution with time of this uncommon, but highly dangerous, type of activity of Villarrica volcano.

Based on lithological and textural features, we divided the Chaimilla deposit into 4 main eruption phases: Basal, Lower, Middle and Upper phases, which consist of several units (units A-J). Both fallout and pyroclastic density current units are present. The dispersal maps of different eruptive units are characterized by a weak variation on the dispersal axis (being the unit C dispersed mainly northward and the unit H north-westward), suggesting a change in wind direction during the eruption.
We estimated the erupted volume of the main fallout units and our results indicate that Chaimilla deposit was generated by a large-magnitude eruption (VEI 4).
Grain size distribution of both Lower and Upper fallout samples show a unimodal distribution, ranging from -5 to 9 , with the fraction >4 (<63 μm) always ≤1 wt%. Unit F (Middle phase) has a slightly bimodal grain size distribution and significant amount of fine ash. Samples from the Basal phase have instead a strongly bimodal grain size distribution, with a predominance of ash fraction. Juvenile component predominates in all the Chaimilla deposit, and lithic content decreases from bottom to top of the deposit, suggesting that the beginning of the eruption was characterized by the opening of a closed vent.

While the grain size distribution of Lower and Upper phase of Chaimilla eruption is always unimodal, density distribution of juvenile samples shows a strong bimodal character, whose bimodality is higher in the Lower phase with respect to the Upper phase. We identified two different clast populations: population 1 is the lightest one, having mode between 1.0 and 1.2 gr/cm^3. Population 2 represents the densest clasts with a mode ranging between 1.4 and 1.8 gr/cm^3. Clast microtextures

are different in the two populations: clasts from population 1 have spherical- to irregular-shaped bubbles and moderately crystallized groundmass (~40 vol%), while population 2 has clasts characterized by strongly irregular to collapsed bubbles and highly crystallized groundmass (~60 vol%).

Our eruption model implies the arrival of new magma (represented by clast population 1) into a stagnant, degassed magma body which was accumulated at shallow level (clast population 2). The new magma body exsolved volatiles that could not easily escape through the conduit due to presence of stagnant body. This caused gas pressure to build up, triggering the explosive eruption. The eruption started with multiple ash-rich explosions leading to vent opening (Basal phase). The following Lower phase marked the onset of the first highly explosive phase of the eruption, with final vent opening and crater widening, as marked by decreasing lithic content from bottom to top of the deposit. The Lower phase deposit was generated by a pulsating, plume column, which instability was probably due to the large amount of the dense clast population 2. The plume column collapsed completely during the Middle phase, which is in fact characterised by series of pyroclastic density current deposits. With the oncoming of the Upper phase, the plume column built up again and remained sustained producing a thick fallout bed predominantly constitued of low-density clast population 1. The eruption ended with thick series pyroclastic density currents which marked the total collapse of the eruptive column.

REFERENCES

Clavero, J. & Moreno, H. 2004. Evolution of Villarica Volcano, in Villarica Volcano (39.5˚S), southern Andes, Chile. In: Lara LE, Clavero JE (eds) Villarrica Volcano (39.5S) southern Andes, Chile. Gobierno de Chile, Servicio Nacional de Geología y Minería, pp 17-27

Gurioli L, Harris AJL, Houghton BF, Polacci M, Ripepe M (2008) Textural and geophysical characterization of explosive basaltic activity at Villarrica volcano. Journal of Geophysical Research 113:doi:10.1029/2007JB005328

Witter JB, Kress VC, Delmelle P, Stix J (2004) Volatile degassing, petrology, and magma dynamics of the Villarrica lava lake, southern Chile. Journal of Volcanology and Geothermal Research, 134, 303-337

3.12

Pumice, a window into the volcanic conduit

Degruyter Wim*, Dufek Josef**, Bachmann Olivier***,*

*Section des Sciences de la Terre et de l'Environnement, 13 Rue des Maraîchers, CH-1205, Genève (wim.degruyter@unige.ch)
**School of Earth and Atmospheric Sciences, 311 Ferst Drive, Georgia Institute of Technology, Atlanta, GA 30332 (USA)
*** Department of Earth and Space Sciences, Mailstop 351310, University of Washington, Seattle, WA 98195-1310 (USA)*

To better understand pumice microtextures and stress distribution within the volcanic conduit, a numerical study is performed using passive tracers to map the type and amount of shear in different parts of the conduit. During an explosive eruption pumices are formed by fragmenting the rising magmatic foam (i.e. highly vesicular magma). Provided they are quenched fast enough, pumices reflect the state of the magma just prior to fragmentation and their microtextures carry information on the stresses applied during magma ascent. Numerous deposits contain both tube pumice, with highly elongated vesicles and frothy pumice, with nearly spherical vesicles showing evidence that they were exposed to different stresses during magma ascent (e.g. Kos Plateau Tuff and Campanian Ignimbrite). The main aim of this investigation is to determine the strain histories of magmatic parcels that eventually become pumice

We have modified the Multiphase Flow with Interphase Exchanges (MFIX) code to simulate a two-phase (bubbles and magma), two-dimensional, isothermal flow with disequilibrium bubble growth. We include a rheology model depending on water content with outlet expansion into the atmosphere. Furthermore, different fragmentation criteria (i.e. critical gas volume fraction, strain rate and gas overpressure) are examined. Strain histories are investigated by releasing passive tracers within simulated magma rise, which record the pure and simple shear strain rates during ascent. The range of accumulated stresses at fragmentation shown by the passive tracers can then be linked to the range of different microtextures found within pumices.

3.13

Hornblende fractionation and peraluminous tonalite: an example of the Chelan Complex, Washington Cascades, USA

Dessimoz Mathias*, Othmar Müntener*

* *Institut de minéralogie et géochimie, Université de Lausanne, 1015 Dorigny (mathias.dessimoz@unil.ch)*

Over the last years numerous experimental studies on the role of H_2O were performed to understand how crustal differentiation occurs at high pressure under water (under)saturated conditions similar to what is expected in island arcs. These experiments emphasize the role of silica poor phases such as garnet and amphibole at high pressure on the differentiation of basaltic melt. Here we present results from a study on the Chelan Complex (Western U.S) to evaluate the role of hornblende in the formation of felsic plutonic rocks.
The Chelan complex is a deep plutonic complex exposed in the North Cascades Core at the southern end of the northwest trending Chelan block. It represents one of the deeper exposures (30 km) of the Cascadian arc and could therefore help to improve our understanding of which processes occur in the deep part of a continental arc and the fractionation processes of wet mafic magmas at high pressure.

The Chelan Complex is composed by tonalite, gabbros, ultramafic rocks and “migmatite”. Field observations, in particular comb layers, pegmatitic gabbros and igneous breccias indicate that the magmatic origin is well preserved along the entire complex. While subsolidus deformation occurs locally, most of the rocks are deformed in presence of a silicate melt, as indicated by a pervasive magmatic foliation well developed in the tonalite as well as some shear zones filled with sillicic melt and few magmatic folds.

The pressure of emplacement of the complex is bracketed between 0.6 Gpa and 1.5 Gpa by the widespread occurrence of primary epidote in tonalite and gabbros and by the absence of garnet. However, the formation of pyroxene spinel symplectites after olivine and plagioclase and Al-Ti systematics in hornblende indicate emplacement pressures of about 1.0 Gpa followed by isobaric cooling to 700°C at 1.0 Gpa.

Idiomorphic amphibole and interstitial plagioclase in gabbros, lack of negative Eu anomaly in amphibole and increase of Zr/Ti suggest early amphibole rather than plagioclase fractionation.

Whole rock chemistry performed on hornblendite, hornblende gabbros, diorite, tonalite and mafic dykes display continuous trends for various oxides and are coherent with an evolution through magmatic processes. The different behaviour of major elements could be reproduced successfully by a simple crystal fractionation model, in agreement with proportion and composition of cumulates observed in the field (ultramafic, hornblendite and gabbros) and mineral composition measured.

Textural observations, modelling and results of high pressure experiments indicate that hornblende is the main phase controlling the differentiation of the Chelan complex at high pressure and high water pressure. We hypothesize that peraluminous tonalite with high Sr/Y could be derived from a basaltic melt by hornblende fractionation and assimilation of crustal material is thus not required.

3.14

Peridotites on Macquarie Island: evidence for anciently-depleted domains in the Earth's mantle pointing to global Proterozoic melting 'events'?

Dijkstra, Arjan H.*

**Institut de Géologie, d'Hydrogéologie et de Géothermie, Université de Neuchâtel, CP 158, 2009, Neuchâtel*

Macquarie Island in the Southern Ocean is a fragment of Miocene ocean crust underlain by mantle peridotites that was uplifted and exposed above sea-level. Petrological and geochemical analysis has shown that the mantle rocks are too refractory to be the source residue of the overlying crustal rocks. For instance, the peridotites contain essentially no residual clinopyroxene, suggesting very high degrees of partial melting and melt extraction. Melting models involving trace elements suggest that the peridotites have seen in excess of 20% near-fractional melting.

Osmium isotope analysis of whole rock samples of peridotites from Macquarie Island yielded very unradiogenic $^{187}Os/^{188}Os$ ratios of 0.1194-0.1229. These values are much lower than typical values obtained on abyssal peridotites. They indicate a long-lived Re-depletion. Re-depletion model ages are Proterozoic (0.7-1.2 Ga). These results confirm that there is no simple genetic link between the Miocene crust and the mantle rocks exposed on Macquarie Island, but that the mantle rocks are a fragment of mantle that has recorded an old melting event, without any subsequent refertilization.

Ultra-refractory peridotites are also known from the 15-20° Fracture Zone (Mid-Atlantic Ridge) and the Izu-Bonin-Mariana fore-arc, and they are found as xenoliths from beneath Kerguelen Island and Hawaii. In all these cases, the ultra-refractory peridotites also gave old Re-depletion ages. The Macquarie Island peridotites are probably samples of an anciently-depleted, ultra-refractory mantle reservoir that has global significance, but that has generally been overlooked so far because of its sterility, i.e., its inability to further produce basalt.

The most tentative aspect of the, admittedly very limited, data-set of Os isotope ratios of ultra-refractory peridotites from the localities listed above is that they seem to point to two global melting events in the Proterozoic, around 0.8 and 1.2 Ga (based on Re-depletion ages). The possible geological significance of these events will be explored in my contribution.

REFERENCES

Dijkstra, A.H., Sergeev, D.S., Spandler, C.A., Pettke, T., Meisel,T., and Cawood, P.A. Ultra-refractory peridotites on Macquarie Island and the case for anciently-depleted domains in the Earth's mantle. Accepted for publication in Journal of Petrology, 2009.

3.15

Sphalerite mineralisation in Bajocian shallow-water carbonates in the Swiss Jura Mountains related to extensional synsedimentary tectonics during the Middle-Late Jurassic.

Natalia Efimenko*, Jorge E. Spangenberg**, Jens Schneider***, Massimo Chiaradia****, Thierry Adatte*, Virginie Matera***** and Karl B. Föllmi*

Institut de Géologie et Paléontologie, Université de Lausanne, 1015 Lausanne, Switzerland (natalia.efimenko@unil.ch)
Institut de Minéralogie et Géochimie, Université de Lausanne, 1015 Lausanne, Switzerland
Département of Earth and Environmental Sciences, Katholieke Universiteit Leuven, Celestijnenlaan 200E, 3001 Heverlee, Belgium
Département de Minéralogie, Université de Genève, 1205 Genève, Switzerland
Institut de Géologie et d'Hydrogéologie, Université de Neuchâtel, 2007 Neuchâtel, Switzerland

Disseminated sphalerite mineralisation occurs in Triassic and Jurassic carbonates in the Swiss Jura Mountains (e.g. Holenweg, 1969; Hofmann, 1989). We report new results from an ongoing study on cadmium-rich (up to 1.8 wt.%) sphalerite (ZnS) found in oolithic carbonates of Bajocian age at Lausen, Auenstein and Pratteln (Canton Basel Land). These oolithic carbonates of the "Hauptrogenstein" formation contain elevated concentrations of Cd (up to 21.4 ppm; Rambeau, 2006) and Zn (up to 207 ppm; Jacquat et al., 2009). We aim to understand how these metals were incorporated into the rock and the conditions of sphalerite formation by using thin-section microscopy, XRD, ICP-MS, LA-ICPMS, EMP, cathodoluminescence, sulphur isotopes, and Rb-Sr/Pb-Pb isotopic dating and tracing.

Cd and Zn enrichments are mostly associated with permeable oolithic carbonate lithologies. High concentrations of Cd and Zn in less permeable rocks (marls, micritic carbonates) appear to be fault-controlled. For example, in marly basinal deposits of the Klingnau Formation (coeval in age to the Hauptrogenstein formation) at Holderbank, Cd concentrations are low at 0,03 ppm but attain up to 0.5 ppm near faults. Likewise, Zn increases from 20 to 300 ppm towards these faults. This Cd and Zn zonation suggests that the circulating fluids were rich in Cd and Zn compared to the primary hostrock, and mainly focussed by faults systems or by permeable rock units.

The distribution of Zn and Cd concentrations in the oolithic carbonate rocks is highly heterogeneous. This appears to be related to porosity differences, and probably to difference in the distribution of Zn- and Cd-bearing phases within the rock. Zinc was shown to be associated with calcite, goethite and sphalerite (Jacquat et al., 2009). Cadmium is most likely adsorbed onto the surface of oolithic carbonate grains (Rambeau, 2006), goethite, clay minerals, pyrite, and within the sphalerite crystals. The preferential correlation of Cd with Zn in carbonate rock may be related to the high concentration of Cd in sphalerite. Nevertheless, Cd concentration does not systematically correlate with Zn. This may be explained by the different behaviour of these two metals during their retention onto mineral phases (goethite, clay minerals, pyrite, carbonate). At

Lausen, Cd concentration decreases from 12 to 0.03 ppm and Zn from 2000 ppm to 12 ppm within few centimetres from reduced grey portions to more altered yellowish parts of the rock. Spalerite microcrystals and framboidal pyrite were observed in grey unaltered parts. No sphalerite was observed in the altered rock portions, where pyrite was oxidized.
This suggests that Cd and Zn were remobilised during the weathering processes.
XRD analyses of sphalerite crystals revealed the presence of both sphalerite and wurtzite. The existence of wurtzite indicates bacterial activity involved in ZnS crystallisation at low temperatures (less than 60-80°). The negative $\delta^{34}S$ values of sphalerites (−22.3 to −5.3‰) point to bacterial sulfate reduction (BSR) as the main source of reduced sulfur. A contribution of sulfide from sedimentary pyrite cannot be excluded.
Direct Rb-Sr dating of selected sphalerite samples from Auenstein yields an upper Middle Jurassic (Bathonian) isochron age of 162 ± 4 Ma which is interpreted to record sphalerite formation during a period of widespread tectonothermal activity related to the opening of the North Atlantic and Tethyan oceans. These syn-sedimentary tectonics also influenced the paleotopography and facies distribution, which were spatially related to reactivated Paleozoic faults (e.g. Allenbach, 2001). Therefore, we propose a model of cadmium and zinc enrichment in the carbonate rocks by deep-sourced fluids during multistage tectonic processes in the region related to an extensional regime during the Jurassic. The Pb isotopic composition of sphalerite is very uniform, indicating an isotopically well-homogenized fluid system. Comparative Pb isotope patterns may point to lead sources located in granitic and metamorphic basement rocks exposed in the southern Black Forest farther north. Lead may have scavenged, mixed and homogenized from Pb-isotopically distinct crystalline basement rock types by fluids during the Bathonian to yield a Pb isotope signature compatible with carbonated-hosted sphalerite in the Swiss Jura.
Sphalerite precipitation may be related to the active bacterial sulphate reduction. The zonation of Cd and Zn in carbonate rocks seems to be controlled by the distribution of facies and the existence of faults. During the Tertiary, tectonic activity in Jura Mountains area may have triggered oxidative alteration of sulfides, formation of iron oxy-hydroxides, and remobilisation of Cd and Zn.

REFERENCES

Allenbach R. P. 2001: Synsedimentary tectonics in an epicontinental sea: a new interpretation of the Oxfordian basin of northern Switzerland. Eclogae Geologicae Helvetiae, 94, 265-287.

Hofmann B. 1989: Erzmineralien in paläozoischen, mesozoischen und tertären Sedimenten der Nordschweiz und Südwestdeutschlands. Schweiz. Mineralogische und Petrographische Mitteilungen, 69, 345-357.

Holenweg H. 1969: Mineralparagenesen im Schweizer Jura. Schweizer Strahler, 3, 303-308.

Jacquat O., Voegelin A., Juillot F. & Kretzschmar R. 2009: Chages in Zn speciation during soil formation from Zn-rich limestones. Geochimica et Cosmochimica Acta, 73, 5554-5571.

Rambeau C. 2006: Cadmium anomalies in jurassic carbonates (Bajocian, Oxfordian) in western and southern Europe. PhD thesis, University of Neuchâtel, 179 p. (unpubl.).

3.16

Modeling the evolution of geothermal reservoirs in deep fractured rocks: Coupling chemistry to heat and fluid transport

Hingerl Ferdinand F. *,**, Wagner Thomas **, Kulik Dmitrii A. *, Kosakowski Georg*, Driesner Thomas**, Thomsen Kaj*** & Heinrich Christoph A. **

Paul Scherrer Institut, 5232 Villigen PSI, Switzerland, (ferdinand.hingerl@psi.ch)
Institute of Isotope Geochemistry and Mineral Resources, ETH Zurich, Switzerland
***Technical University of Denmark, 2800 Kgs. Lyngby, Denmark*

A consortium of research groups from ETH Zurich, the Paul Scherrer Institut, EPF Lausanne, and the University of Bonn, cooperate in the **CCES** program **GEOTHERM** (www.geotherm.ethz.ch) aimed at performing basic research on key aspects of Enhanced Geothermal Systems (EGSs). Our task within the program consists of modeling the fluid–rock interaction and scale formation during geothermal heat extraction. In particular, we are developing advanced software that should realistically simulate the long term (years to decades) evolution of the permeability and heat exchange efficiency in an EGS reservoir.

Our simulations are anchored on theoretical investigations of the interplay of chemical processes (mineral dissolution and precipitation in rock fractures and technical installations) with the flow of the reactive fluid through a geometrically complex and changing fracture network. Modeling of this integrative scenario is performed by coupling a chemical equilibrium

solver with algorithms that simulate the mass and heat transport and geometrical phenomena. The chemical solvers are commonly based on a Law-of-Mass-Action (LMA) method, whereas in our work, the complementary Gibbs-Energy-Minimization (GEM) code package GEM-Selektor (http://gems.web.psi.ch) is used. GEM chemical solvers can compute phase speciation in more chemically plausible systems than it can be done using LMA solvers, especially when many highly non-ideal solutions are involved.

The EGS reservoir is characterized by variable (up to high) salinity and elevated temperature and pressure, which is a challenge on the calculation of aqueous speciation. For this reason, in addition to several variants of Debye-Huckel equation, we have implemented the Pitzer (Harvie et al. 1984) and the EUNIQUAC (Thomsen & Rasmussen 1999) aqueous activity model, both applicable to mixed electrolyte systems at high ionic strength. Compared with the conventional Pitzer model, EUNIQUAC requires fewer empirical fit parameters (only binary interaction parameters needed) and uses simpler and more stable temperature and pressure extrapolations. This results in an increase in computation speed, which is of crucial importance when performing coupled long term simulations of geothermal reservoirs.

In order to successfully apply the implemented electrolyte solution models, we are currently compiling a thermodynamic database and extend it with relevant Pitzer and EUNIQUAC parameters for calculating mineral solubility in a wide range of temperatures, pressures and ionic strength as applicable to geothermal fluids. We have also implemented the Soave-Redlich-Kwong (Soave 1972) and Peng-Robinson (Peng and Robinson 1976) equations of state for non-ideal gas mixtures, which will enable simultaneous calculations of gas solubility and boiling processes.

The standalone GEM numerical kernel of the GEM-Selektor code (abbreviated GEMIPM2K) was already successfully coupled to the Thermo-Hydro-Mechanical (THM) code GeoSys/Rockflow (Shao et al. 2009). Further coupling with the advanced TH code CSMP++ (Coumou 2008; http://csmp.ese.imperial.ac.uk/wiki/Home) is foreseen within the project. The novel coupled codes utilizing GEMIPM2K will be used within a benchmarking study, testing the efficiency, the numerical stability, and the sensitivity of the results to different numerical procedures and geochemical approaches, last but not not least to the impact of the choice of a thermodynamic data set. As the concluding step, we intend to construct a conceptual model for the geochemical water-rock interaction processes including the formation of mineral scales and the corrosion of pipes in wells at the Basel EGSs site.

REFERENCES

Bruno J., Bosbach D., Kulik D., Navrotsky A. 2007: Chemical thermodynamics of solid solutions of interest in radioactive waste management:A state-of-the art report, Chemical Thermodynamics Series, 10, Paris, OECD, 266 p.

Coumou, D. , **Matthäi, S., Geiger , S., and Driesner, T.** 2008. Computers & Geoscience, Volume 34, Issue 12, pp 1697-1707

Harvie, E.H., Moller, N., Weare, J.H. 1984. The prediction of mineral solubilities in natural waters: The Na-K-Mg-Ca-H-Cl-SO_4-OH-HCO_3-CO_3-CO_2-H2O systemto high ionic strengths at 25°C. Geochim. Cosmochim. Acta Vol. 48, pp. 723-751.

Karpov, I.K., Chudnenko, K.V., Kulik, D.A. 1997. Modeling chemical mass transfer in geochemical processes: thermodynamic relations, conditions of equilibria, and numerical algorithms. American Journal of Science 297: 767-806.

Karpov I.K., Chudnenko, K.V., Kulik, D.A., Avchenko, O.V., and Bychinski, V.A. 2001. Minimization of Gibbs free energy in geochemical systems by convex programming. Geochemistry International 39, no. 11: 1108-1119.

Kulik, D., Berner, U., and Curti, E. 2004. Modelling chemical equilibrium partitioning with the GEMS-PSI code. In: PSI Scientific Report 2003 / Volume IV, Nuclear Energy and Safety (Eds. B.Smith and B.Gschwend), Paul Scherrer Institut, Villigen, p.109-122.

Kulik D.A. 2006a. Classic adsorption isotherms incorporated in modern surface complexation models: Implications for sorption of actinides. Radiochimica Acta 94, no. 9-11: 765-778.

Peng, D.Y., Robinson, D.N. (1976) A new two-constant equation of state. INd. Eng. Chem. Fundam., 15, 59-64.

Soave, G. (1972) Equilibrium constants from a modified Redlich-Kwong equation of state. Chem. Eng. Sci. 27, 1197-1203.

Shao, H., Dmytrieva, S. V., Kolditz, O., Kulik, D. A., Pfingsten, W., Kosakowski, G. 2009. Modeling reactive transport in non-ideal aqueous - solid solution system. Applied Geochemistry 24, 1287-1300.

Thomsen, K., Rasmussen, P. 1999. Modeling of Vapor-Liquid-Solid Equilibria in Gas – Aqueous Electrolyte Systems. Chem. Eng. Sci., 54, 1787-1802.

3.17

The mafic – granitic connection of the Torres del Paine laccolith, Patagonia

J. Leuthold1, O. Müntener1, L. Baumgartner1, B. Putlitz1, M. Ovtcharova2, Urs Schaltegger2, Massimo Chiaradia2

1 IMG-UNIL, CH-1015 Lausanne, Switzerland (julien.leuthold@unil.ch)
2 Mineralogy – UNIGE, CH-1205 Geneva, Switzerland

We have conducted a field, petrological and geochronological study of a bimodal intrusive complex from the Torres del Paine laccolith, Patagonia, Chile. The goal of this study is to understand how various types of mafic rocks evolve at shallow pressure and how they are related in space and time to the various granitic sheets. From field relations it is evident that the granite intruded as a series of sheets, with the oldest pulse on top and the youngest at the base of the laccolith. High precision U-Pb dating on single zircons (Michel et al. Geology 2008) is in agreement with field relations and yielded 12.59±0.02 for the oldest and 12.51±0.03 for the youngest granite dated.
The granites are underlain by a series of mafic sills composed of hornblende-gabbros and diorites. We distinguish two types of hornblende gabbros that are chemically similar but clearly different with respect to their mineral crystallization sequence. However, the contacts between the different mafic rocks are ductile as illustrated by mafic enclaves in diorite or ascent of small diorite diapirs into overlaying hornblende gabbros, indicating (near-) simultaneous emplacement of most of the mafic rocks.
Bulk rock chemistry suggests that the mafic and granitic rocks follow a high – K calcalkaline to shoshonitic differentiation trend. Liquid compositions calculated from Laser Ablation ICP-MS trace element analysis of cumulate minerals indicate that the mafic rocks crystallized from a K-rich basaltic to shoshonitic magma. Intercumulus minerals show equilibrium with a granodioritic to granitic melt, that is similar to Paine granites. Preliminary isotope dilution – thermal ionization mass spectrometry on zircons from one gabbro and one diorite yielded 12.40±0.04 and 12.447±0.013 Ma, which is about 60'000 years younger than the youngest granite dated so far. This would suggest that a large volume of the laccolith grows downwards, with younger and more mafic sheets at the bottom of the complex. The youngest granites that cut the entire complex, however, await precise dating.

REFERENCES
Michel et al. (2008), Geology 36/6, 459-462

3.18

Bromine speciation and partitioning in high pressure aqueous fluids and silicate melts: implication for the behavior of halogens in subduction zones

M. Louvel*, C. Sanchez-Valle*, W.J. Malfait*, G.S. Pokrovski**, C.N. Borca***, D. Grolimund***

**Institute for Mineralogy and Petrology, ETH Zurich, CH-8092 Zurich, Switzerland. (marion.louvel@erdw.ethz.ch)*
***CNRS, Laboratoire des Mecanismes et Transferts en Geologie, F-31400 Toulouse, France.*
****Swiss Light Source, CH-5232 Villigen PSI, Switzerland.*

Although halogens are minor volatiles in the Earth's crust, they are important tracers of magmatic and degassing processes and provide insights about subsurface magma movement and eruption likelihood in subduction-related volcanism [1]. Additionally, their ability to complex with other elements has also considerable implications on the formation and distribution of ore deposits [2]. Prerequisite for an efficient use of halogens as geological tracers is an adequate knowledge of their solubility and distribution between aqueous fluids and silicate melts, as well as their speciation in subduction zone fluids. Experimental data on the solubility and fluid-melt partitioning behavior of halogens is however limited to pressures below 0.3 GPa [3,4] and virtually no data is available on their speciation in high-pressure fluids.
In order to investigate the behavior of halogens in sub-arc environments, X-ray absorption (XAFS) and X-ray fluorescence (XRF) spectroscopy measurements were conducted in a hydrothermal diamond-anvil cell (HDAC-[5]) up to 850 °C and 1.5(1) GPa in Bromine-rich fluids equilibrated with silicate melts. Bromine was used as an analog for chlorine suitable for X-ray fluore-

scence measurements through the diamond windows of the HDAC. Experiments were conducted at the X05-LA MicroXAS beamline of the Swiss Light Source (Switzerland). Pressure in the sample chamber was monitored from the PVT equation of state of a chip of gold added to the experimental volume. Br fluid-melt partition coefficients in the haplogranite-H_2O system were determined by XRF spectroscopy. Br speciation was investigated using XAFS over a wide range of P-T and bulk compositions, ranging from pure NaBr aqueous solutions (3wt% Br) to alkali-SiO_2-rich solutions, water-saturated $Na_2Si_2O_5$ and haplogranititic melts and supercritical fluids (25wt% $Na_2Si_2O_5$ and 10wt% haplogranite).
The combined results of these experiments provide valuable information on the partitioning behavior and structural environment of Br in high-pressure fluids. Br strongly partitions into the aqueous fluid phase, in agreement with the results of Bureau et al. [6] in quench experiments. Partition coefficients $D^{fluid/melt}$ are close to 25 at 650 °C – 1.0(1) GPa but decrease with increasing P-T, as the system approaches miscibility. The XAFS data reveal changes in the local structure around Br as chemical complexity increases in the system from NaBr solutions to alkali-rich SiO_2 fluids, suggesting the complexation of Br with Na, Si and Al. The implications of these results for the behavior of Br and halogens in subduction zone fluids will be discussed.

REFERENCES
[1]Aiuppa et al (2008), Chem. Geol. 263, 1-18.[2]Hedenquist&Lowenstern (1994), Nature 370, 519-527.[3]Webster (1992), Geoch. Cosmo. Act. 56, 679-687.[4]Bureau&Metrich (2003), Geoch. Cosmo. Act. 67, 1689-1697.[5]Bassett et al (1993), Rev. Sci. Inst. 64, 2340-2345.[6]Bureau et al (2000), Earth. Planet. Sci. Lett. 183, 51-60.

3.19

Compositional dependent compressibility of dissolved water in silicate glasses revealed by Brillouin scattering on haplogranitic and basaltic glasses

Wim J. Malfait*, Carmen Sanchez-Valle*, Paola Ardia*,** & Etienne Médard***

*Institute for Mineralogy and Petrology, ETH Zurich, CH-8092 Zurich (wim.malfait@erdw.ethz.ch)
**Dept. of Geology and Geophysics, University of Minnesota, MN 55455 Minneapolis, USA
***Laboratoire Magmas et Volcans, Université Blaise-Pascal-CNRS, OPGC, F-63038 Clermont-Ferrand

The density of hydrous magmas is a key control on the timescales and outcome of many igneous processes, *e.g.* the crystal settling velocities in a magma chamber and the emplacement depth of intrusions. Unfortunately, direct density measurements on hydrous liquids at magmatic temperatures and pressures are experimentally challenging and as a result, very few experimental data are available. At atmospheric pressure and room temperature, the partial molar volume of water in silicate glasses and melts seems to be independent of the bulk composition of the glass (Richet and Polian, 1998). Encouraged by this constant partial molar volume at room conditions and because of the lack of sufficient experimental constraints, current density models for hydrous magmatic liquids (*e.g.* Ochs and Lange, 1999) assume that the partial molar volume of the dissolved water at high temperature and pressure is also independent of melt composition. This assumption, however, has never been experimentally confirmed.

In order to verify if the partial molar volume of water remains independent of magma composition at elevated pressures, we have determined the sound wave velocities and bulk modulus (K_S) of a series of hydrous haplogranitic and basaltic glasses, quenched at different pressures, using Brillouin spectroscopy. The compressional wave (V_P) and shear wave velocities (V_S) systematically decrease with the addition of water. The partial molar K_S of water, and hence the compressibility, is different for different magma compositions. This implies that the partial molar volume of water will not be independent of melt composition at elevated pressure. These results suggest that the density model of Ochs and Lange (1999) may have limited applicability at elevated pressure. The development of more robust density models for hydrous magmatic liquids cannot proceed until additional in situ, high pressure and temperature measurements of melt density, thermal expansion and/or compressibility are available.

REFERENCES
Ochs, F.A., and Lange, R.A. (1999) The density of hydrous magmatic liquids. Science, 283, 1314.
Richet, P., and Polian, A. (1998) Water as a dense icelike component in silicate glasses. Science, 281, 396-398.

3.20

PVTx properties of high pressure aqueous fluids by Brillouin scattering spectroscopy

Mantegazzi Davide*, Sanchez-Valle Carmen*, Reusser Eric*, Driesner Thomas**

*Inst. for Mineralogy and Petrology, ETH Zurich, CH-8092 Zurich, (davide.mantegazzi@erdw.ethz.ch)
** Inst. of Isotope Geochemistry and Mineral Resources, ETH Zurich, CH-8092 Zurich

Aqueous fluids play a very important role in many geological processes in the Earth's crust and mantle. Typical examples of fluid mediated geological events are: the magma production in the mantle wedge beneath active volcanoes at subduction zones, metamorphic reactions involving fluid phases, the hydrothermal alteration of the seafloor, the transport of chemical components and the related ore deposits formation.

Studies on Fluid Inclusions (FI) have pointed out that fluids in the ternary system H_2O – NaCl – CO_2 can be considered as good approximation for natural geological fluids.

In order to quantitatively model fluid-rock interactions, thermodynamic data on minerals and fluids at geologically relevant P-T conditions are necessary. While these data are available for the most rock-forming minerals, this is not the case for aqueous fluids different than pure H_2O. For example, the equations of state (EoS) of H_2O – NaCl fluids are restricted to 0.5 GPa. Therefore, the interpretation of fluid related deep geological processes requires the extrapolation of thermodynamic properties over an order in magnitude in pressure. In addition, the knowledge of the thermodynamic properties of fluids in the ternary system H_2O – NaCl – CO_2 is essential for understanding and modeling the FI data.

In this contribution we present the PVTx properties of different aqueous fluids up to high P-T conditions, calculated from sound velocity measurements using Brillouin scattering spectroscopy. All experiments were conducted in an externally heated membrane-type diamond anvil cell (mDAC).

Brillouin scattering spectroscopy allows the direct measurement of the velocity of acoustic waves propagating in a material (fluid or solid). The collected sound velocities V_p are used to determine the EoS (P, T,x) of the analyzed fluids.
The results are combined with previous experimental and theoretical EoS to obtain a continuous model from low to high P-T conditions, providing a database for the thermodynamic properties of the most relevant aqueous systems involved in fluid-mediated geological processes.
Figure 1 shows the comparison between the EoS (P, T,x) of different H_2O – NaCl mixtures. At 2 GPa the solution with 5.5 wt% NaCl is 5.2% denser than pure water, while at 3 GPa the solution with 14.9 wt% NaCl is 9.6% denser than water. With increasing pressure the difference in density between water and chloride-rich solutions is increasing.

REFERENCES

Abramson, E., & Brown, M.J. 2004: Equation of state of water based on speeds of sound measured in the diamond-anvil cell. Geochim. Cosmochim. Acta 68, 1827-1835.

Driesner, T. 2007: The system H2O-NaCl. Part II: Correlations for molar volume, enthalpy, and isobaric heat capacity from 0 to 1000 degrees C, 1 to 5000 bar, and 0 to 1 X-NaCl. Geochim. Cosmochim. Acta 71, 4902-4919.

Sanchez-Valle, C., & Bass, J. D. 2007: Equation of state of fluids from sound velocity measurements in the diamond anvil cell using Brillouin scattering spectroscopy. Geochim. Cosmochim. Acta 71, A873-A873.

Wagner, W., & Pruss, A. 2002: The IAPWS formulation 1995 for the thermodynamic properties of ordinary water substance for general and scientific use. J. Phys. Chem. Ref. Data 31, 387–535.

Figure 1. EoS (P, T, X) for H2O – NaCl mixtures with different salt concentrations as a function of pressure along the 200°C isotherm. All these EoS have been determined with the same experimental technique. Data for the 14.9 and 5.5 wt% NaCl solutions are from this work; densities for the 0 wt% NaCl mixture are taken from Sanchez-Valle and Bass (2007).

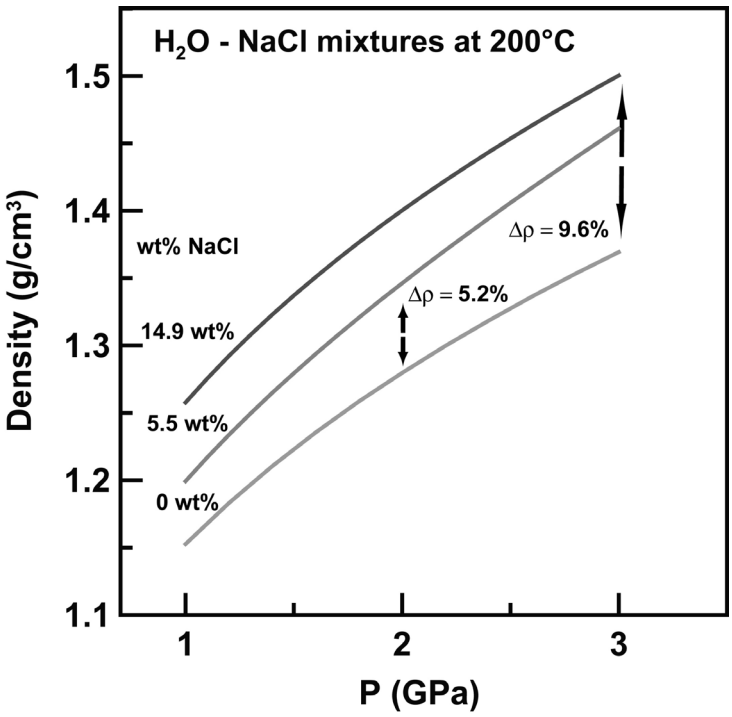

3.21

Evidence of Jurassic rifting in the Dent Blanche nappe (near Cignana, Italy)

Paola Manzotti*, Daniele Regis*, Benedicte Cenki-Tok*, Martin Robyr*, Tonny B. Thomsen*, Daniela Rubatto**, Michele Zucali*** & Martin Engi*

*University of Bern, Baltzerstrasse 1+3, 3012 CH-Bern (manzotti@geo.unibe.ch)
**The Australian National University, Mills road, Canberra, ACT, 0200 Australia
***Dipartimento di Scienze della Terra «Ardito Desio», Università degli Studi di Milano, via Mangiagalli 34, 20133 I-Milano

The Roisan Zone is considered to be the Mesozoic metasedimentary cover of the Dent Blanche nappe (Austroalpine domain, Western Italian Alps; Diehl et al., 1952). It is dismembered into metric to hectometric bands and pods of marbles, dolomitic breccias with a phyllitic matrix, calcschist, micaschist, chlorite schist, impure and manganoan quartzites.

In the Roisan Zone we found the Alpine record to be heterogeneous; the metamorphic imprint indicates low temperature and intermediate pressure, locally this is associated with superimposed mylonitic foliations. Four evolutionary stages have been reconstructed by meso- and microstructural analysis. Pre-stage 1 is a pre-Alpine event recognised only at the microscale. During stage 1 a well differentiated millimetric foliation develops, whereas D2 structures consist of isoclinical folds, transposing the S1 foliation into a new, pervasive S2. D3 structures mainly consist of isoclinal folds: this stage is not always associated with the development of a new foliation.

Within the Roisan Zone, particularly near Cignana, we investigated cross-cutting relationships between metamorphic and deformational signatures. In Mn-quartzite and marble a relative temporal sequence was deduced. Titanite and allanite were singled out for U-Th-Pb dating. Allanite from Mn-quartzites occurs as subhedral crystals and displays irregular zoning in LREE, Ca, Fe, and Mg. SHRIMP and LA-ICP-MS analyses did not yield the metamorphic Alpine age expected on the basis of petrographic and structural observations. The analyzed generation of allanite grains shows Permian ages (between 350 and 290 Ma).

Titanite in marble occurs as abundant subhedral to anhedral crystals (mostly fractured and/or deformed), locally sub-parallel to the foliation. BSE images, qualitative X-ray elemental maps, and EMP spot analysis show weak regular to irregular zoning in Al, Ti and Ca. SHRIMP U-Pb analysis of titanite domains with various Al contents yield apparent spot $^{206}Pb/^{238}U$ ages scattering between 284 and 160 Ma.

The younger ages of titanite are tentatively interpreted as reflecting an extensional regime that preceded the Alpine collision. Further work is underway now to clarify whether zoning of LREE, Ca, Fe and Mg in allanite and variations of Al, Ti and Ca in titanite grains may partly reflect changes in fluid compositions in a metasomatic-hydrothermal system associated with extension, possibly in an oceanic environment.

REFERENCES

Diehl, E.A., Masson, R., Stutz, A.H. 1952: Contributo alla conoscenza del ricoprimento della Dent Blanche. Memorie degli Istituti di Geologia e Mineralogia dell'università di Padova 17, 1-52.

3.22

Ore fluid evolution in a volcanic-hosted epithermal ore deposit: Farallón Negro, Argentina.

Márquez-Zavalía, M. Florencia*, Heinrich, Christoph A.**, Meier, Dimitri**

*IANIGLA, CCT Mendoza, CONICET, CC 330, (5500) Mendoza, Argentina (mzavalia@mendoza-conicet.gov.ar)
**Isotope Geochemistry and Mineral Resources, Federal Institute of Technology, ETH Zentrum NO, CH-8092, Zurich, Switzerland

The Farallón Negro mineral deposit is located in Catamarca province, Argentina, at 27º19´S and 66º40´W. This low sulfidation epithermal gold deposit belongs to the Farallón Negro mining district, along with other epithermal (e.g., Capillitas, Cerro Atajo) and porphyry deposits such as Bajo de la Alumbrera and Agua Rica. This cluster of Cu-Au mineral deposits are genetically linked to a Miocene volcanic complex with a suite of rocks of high-K calk-alcaline to shoshonitic affinities known as Farallón Negro Volcanic Complex (FNVC). Many authors interpreted the whole complex as the remnant of a large andesitic volcano (e.g., Halter et al., 2004; Proffett, 2003; Ulrich et al., 2002; and references therein), though Harris et al. (2006) present some contradicting evidences.

Alto de la Blenda area, where this study was focused, is one of the two main suits of veins of the Farallón Negro mineral deposit. The main veins of Alto de la Blenda are: Laboreo, Esperanza and Esperanza SE. The W part of Laboreo vein is hosted in andesite and the rest of that vein and the other two are hosted in monzonite. They are more than 1000 m long, 1 to 6 m wide, with grades up to 7 g/t Au and 200 g/t Ag (Montenegro & Morales, 2004).

There were recognized four stages of the mineralization with 7 generation of quartz. **Stage I** is represented by the earliest quartz recognized (Q1) in the deposit, present as fragments in a breccia, it is bluish grey in colour and occurs along with fragments of whitish carbonate (Cb1) and scarce disseminated pyrite. **Stage II** corresponds to the breccia, which is cemented by a second generation of quartz (Q2), grey in colour, interlayered with bands of creamy carbonate (Cb2) and associated with free Au, sulphides (pyrite, galena, chalcopyrite, sphalerite) and Cu, Ag, Au and Pb sulphosalts. At the end of this stage, quartz (Q3) in colourless crystals up to 1 cm long fills the remaining open spaces and vugs. **Stage III** is represented by a younger generation of grey quartz (Q4), associated with pink and yellowish carbonate (Cb3) and chalcopyrite and Ag minerals. It occurs parallel to the breccia and frequently crosscutting it. At the end of this stage, small cavities are filled with quartz crystals (Q5) that frequently develop a layered base on which grow transparent, colourless crystals up to 2 cm long, developing comb textures. In some areas, **Stage IV** is present, where the last two generations of quartz can be recognized. The first one (Q6) is scarce and occurs with white (and pink?) layered carbonate (Cb4), mostly oxidized (cryptomelane and pyrolusite >> manganite, manjiroite and "wad") and galena, chalcopyrite and sphalerite generally scarce. Sometimes the association Q6+Cb4 is parallel to the whole sequence and other times crosscuts it. The youngest quartz (Q7) fills the open spaces and develops colourless crystals up to 1 cm long. In several areas of the deposit, localized brecciation affects different parts of the sequence.

Preliminary fluid inclusion results give ranges of homogenization temperatures from 200 to 270ºC, and salinities from 3.40 to 4.70 NaCl equiv. for Esperanza vein and similar homogenization temperatures but lower salinities for Laboreo vein. The first results of microanalyses by LA-ICPMS, performed in primary aqueous fluid inclusions trapped in quartz, show concentrations of ppm-levels of Au and hundreds of ppm of Cu. The highest values of Au concentrations were found in Q2 and Q3, belonging to the second stage of the mineralization, while the highest Cu values came from samples with Q6 and Q7, corresponding to the last stage of the mineralization (Stage IV). Other ore forming elements were also analyzed and all results will be informed in detail when the study is completed. There were as well investigated the aqueous fluids of the late veins, with Au-Ag-bearing quartz+Mn-carbonate+base-metal minerals, found in the Bajo de la Alumbrera open pit (Meier, 2008; Meier et al. 2008) Though the results are still preliminary, the research in progress shows the first saline epithermal fluids in a low-to

intermediate sulfidation epithermal system containing significantly higher metal concentrations than fluids in any active geothermal system (e.g., Simmons and Bronwn, 2006). These very high metal concentrations (ppm-levels of Au and hundreds of ppm of Cu) in the fluid indicate that even low- to intermediate-sulfidation economic vein deposits do not form from convecting groundwater alone, but from injection of vapor-derived magmatic fluid.

REFERENCES

Halter, W.E., Bain, N., Becker, K., Heinrich, C.A., Landtwing, M., VonQuadt, A., Clark, A.H., Sasso, A.M., Bissig, T. & Tosdal, R.M. 2004: From andesitic volcanism to the formation of a porphyry Cu-Au mineralizing magma chamber: the Farallon Negro Volcanic Complex, northwestern Argentina: Journal of Volcanology and Geothermal Research, 136, 1-30.

Harris, A.C., Bryan, S.E. & Holcombe, R.J. 2006: Volcanic setting of the Bajo de la Alumbrera porphyry Cu-Au deposit, Farallon Negro Volcanics, Northwest Argentina: Economic Geology, 101, 71-94.

Meier, D. 2008: Low salinity fluids at the Bajo de la Alumbrera porphyry Cu-Au deposit, Argentina. MSc thesis. Inst. Isotope Geochemistry and Mineral Resources, Dept. Earth Sc., ETH-Zürich, Swiss Federal Institute Technology.

Meier, D. , Heinrich, C.A., Guilong, M. & Márquez-Zavalia, M.F. 2008: Low salinity fluids at the Bajo de la Alumbrera porphyry Cu-Au deposit, Argentina. Swiss Geoscience Meeting.

Montenegro, N. & Morales, F. 2004: Distrito mineralizado Farallón Negro. YMAD, Belén, Catamarca, Argentina. In: Márquez-Zavalía, M.F. (Ed.) Curso Latinoamericano de Metalogenia UNESCO-SEG 2004. Guía de Campo: 83-99.

Proffett, J.M. 2003: Geology of the Bajo de la Alumbrera porphyry copper-gold deposit, Argentina: Economic Geology, 98, 1535-1574.

Ulrich, T., Günther, D. &Heinrich, C.A. 2002: The Evolution of a porphyry Cu-Au deposit, based on LA-ICP-MS analysis of fluid inclusions: Bajo de la Alumbrera, Argentina: Economic Geology, 97, 1889-1920.

Simmons, S.F. & Bronwn, K.L. 2006: Gold in magmatic hydrothermal solutions and the rapid formation of a giant ore deposit. Science, 314, 5797, 288-291.

3.23

Baggalútar from Hvalfjörður, SW Iceland: Volcanic spherulites or not?

Mattsson Hannes B.*, Reusser Eric*

**Institute for Mineralogy and Petrology, Department of Earth Sciences, ETH Zürich, Clausiusstrasse 25, CH-8092 Zürich (hannes.mattsson@erdw.ethz.ch)*

Baggalútar form well-rounded spherules, ranging between 0.5-3 cm in diameter, and occur either as single spherules or aggregates containing up to 10 individual spherules joined together. They are relatively common on beaches along the Atlantic coast in Hvalfjör ur (SW Iceland).In literature, Baggalútar have commonly been explained as being volcanic spherulites (Saemundsson and Gunnlaugsson, 1999). However, Baggalútar lack the internal structure characteristic for volcanic spherulites which commonly involves radial growth of feldspar and quartz needles as silicic glass devitrifies. They are not accretionary lapilli as these commonly form by accretion of fine ash around a nucleii in an onion-like texture. Neither are they consistent with being marine concretions, which are characterized by concentric internal textures.

In thin section, only random internal texture can be observed and the Baggalútar is composed of a fine-grained groundmass with abundant rounded voids which have been infilled with secondary minerals (mainly thomsonite, heulandite and natrolite). XRD and SEM analyses show that the groundmass is composed of lath-shaped plagioclase (An-rich), augitic clinopyroxene and titanomagnetite in various proportions (Fig.1). The overall mineralogy of the Baggalútar is therefore consistent with being basaltic. Furthermore, the internal texture suggests that it could be basaltic ash, in which the vesicles have been infilled by zeolite minerals at a later stage.

However, a few things about the occurrence of Baggalútar remain enigmatic:

1. Absence of phenocrysts. In five investigated thin sections only two small clinopyroxene phenocrysts could be found, and all spherules have a fine-grained homogeneous texture strongly reminiscent of quenching.
2. What causes the well-rounded shape? This is in contrast to the randomly oriented internal structure of the spherules. If only single Baggalútar are considered, their well-rounded shapes could potentially be attributed to marine abrasion. However, this does not explain the occurrence of multi-spherule aggregates in which each spherule is well-rounded.
3. Where do they come from? So far no outcrop has been found in Hvalfjör ur in which the Baggalútar occurs in situ, and finding such an outcrop may help to shed light on their formation.

REFERENCES
Saemundsson, K. & Gunnlaugsson, E. 1999: Islenska steinabokin, Mal og Menning, Reykjavik, pp. 233.

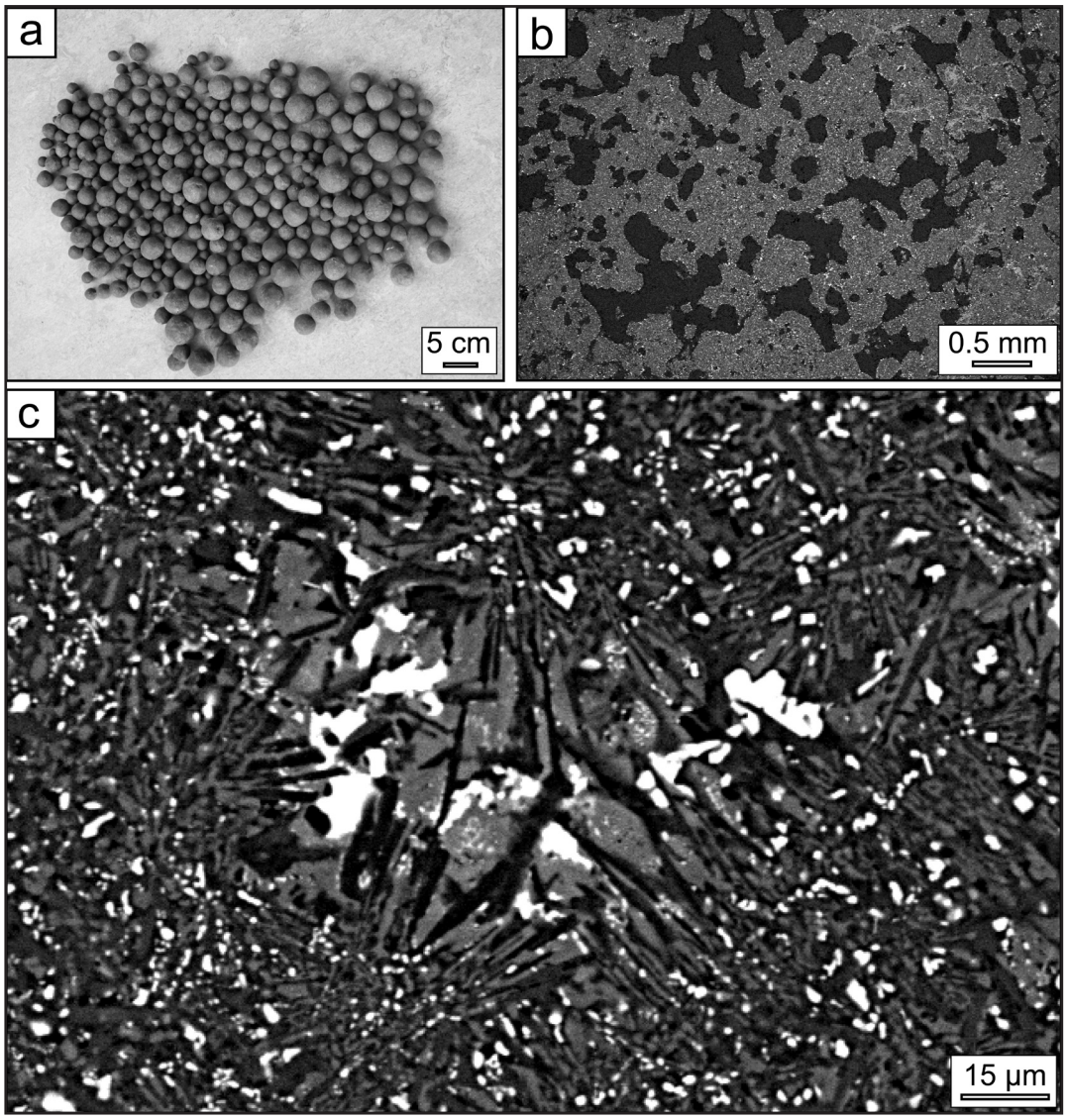

Fig. 1. Characteristics of Baggalútar at different magnifications. (a) A collection of hand specimens. (b) SEM image showing homogeneous internal texture with vesicles infilled by zeolites. (c) Close-up SEM image of the groundmass comprising plagioclase (lath-shaped, dark), clinopyroxene (grey) and titanomagnetite (white).

3.24

Columnar jointing and the formation of "chisel-marks" in the Hrossadalur lava flow, northern Iceland

Mattsson Hannes B.*, Bosshard Sonja*

Institute for Mineralogy and Petrology, Department of Earth Sciences, ETH Zürich, Clausiusstrasse 25, CH-8092 Zürich (hannes.mattsson@erdw.ethz.ch)

Columnar jointing and "chisel-marks" are common features in thick, slowly cooled, basaltic lavas. The fracturing to form columnar jointing is commonly attributed to thermoelastic strain creating a local tensile stress, which results in the formation of joints organized into columns with a polygonal cross-section and large aspect ratio (length/diameter).The chisel marks, on the other hand, are striae oriented perpendicular to the main axis of the column and reflects a stepwise crack propagation as the lavas cool.

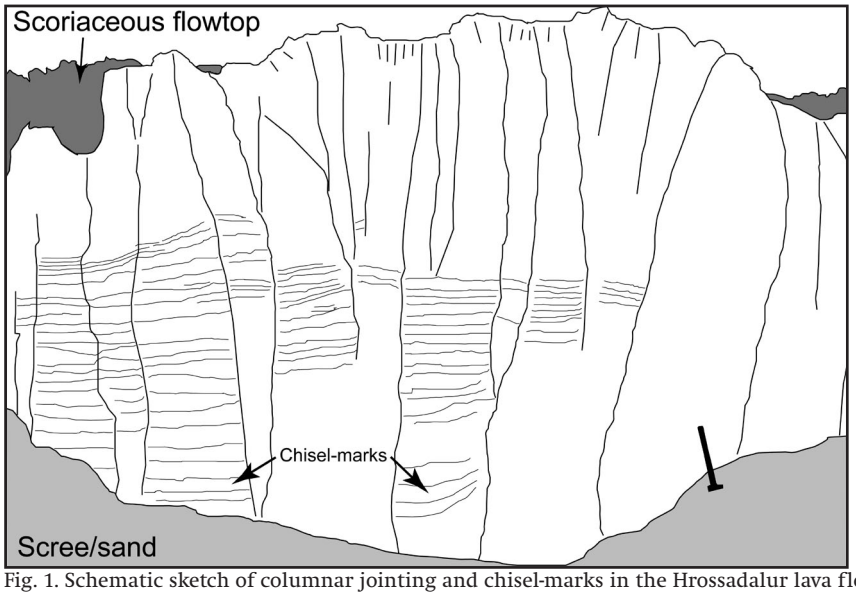

Fig. 1. Schematic sketch of columnar jointing and chisel-marks in the Hrossadalur lava flow. Hammer for scale.

At Hrossadalur in northern Iceland a 200 m long cross-section of a ponded, columnar-jointed, basaltic lava flow is exposed in a normal fault belonging to the much larger Krafla fissure swarm. The total thickness of the Hrossadalur lava flow exceeds 10 m, and display an internal morphology characteristic for p-type pahoehoe with a vesicular upper crust and a dense interior. Close to the top of the lava flow small-scale columnar jointing is abundant (although poorly developed). In this part of the flow chisel marks are absent. Starting roughly 0.8-1.5 m from the top of the flow (i.e. the cooling surface), columnar joints are fewer and larger in size and chisel-marks start to form (Fig. 1). The initial spacing between individual chisel marks is small (a few cm). However, the spacing of the chisel-marks shows a systematic increase with depth into the interior of the flow (in cases exceeding 25 cm near the central part of the flow). The base of the exposed section is composed of a massive part, where columnar jointing and chisel marks are absent. Instead concentric arrangement of vesicles and flow foliation indicate that this portion of the lava flow was occupied by lava tubes.

Measurements of the spacing of chisel-marks at Hrossadalur, in combination with observations of crack propagation in active Hawaiian lava flows (Hon et al., 1994), suggests that the spacing represents the effective thickness of the viscoelastic part of the crust as a lava flow progressively cools and solidifies. The fracture propagation is incremental, going from the brittle crust (<800°C), through the viscoelastic layer (800-1070°C), to the molten interior (>1070°C). After one step of fracture propagation, the flow needs to cool to build up sufficient thermoelastic strain to promote another cycle of crack-propagation.

Tentative modeling of conductive cooling (Carslaw and Jaeger, 1959) involving a change of state (molten to solid), shows good agreement between the time-dependant thickness of viscoelastic crust and the measured spacing of chisel-marks at Hrossadalur. Thus, the spacing of the chisel marks present in columnar jointed basalts can effectively be used to constrain the cooling history of slowly solidifying lava lakes and intrusions as well as lava flows.

REFERENCES

Carslaw, H.S. & Jaeger, J.C. 1959: Conduction of heat in solids, 2nd Ed., Oxford Univ. Press, New York, pp. 510

Hon, K., Kauahikaua, J., Denlinger, R. & Mackay K. 1994: Emplacement and inflation of pahoehoe sheet flows: Observations and measurements of active lava flows on Kilauea volcano, Hawaii, Geological Society of America Bulletin, 106, 351-370.

3.25

Convective instabilities in Volcanic Clouds

Monnard Hélène*, Manzella Irene*, Jeremy Phillips**, Costanza Bonadonna*

*Department of Mineralogy, University of Geneva, Rue des Maraîchers 13, CH-1205 Genève (hmonnard@gmail.com)
**Department of Earth Sciences, Centre for Environmental and Geophysical Flows, University of Bristol, UK

Convective instabilities driven by particle sedimentation may play an important role in the particle dispersal from volcanic plumes (e.g. Figure 1). Such instabilities occur in density stratified fluids and they are characterised by the formation of fingers. When a particle laden fluid is situated above a denser fluid, the two layers are initially stable. With the particle settling, a thickening interface layer becomes gravitationally unstable and fingers could start develop.
Many experiments have been carried out to characterize this process (e.g. Chen 1997; Hoyal et al. 1999; Völtz et al 2000). However, not many experiments were carried out to investigate convective instabilities in a volcanic setting (e.g. Carey 1997). In addition, numerical models used to describe tephra dispersal do not account for convective instabilities.
We have performed laboratory experiments to investigate the dynamics of this phenomenon and its effects on the rate of particle sedimentation from the bottom of the volcanic plume and deposition at the bed.

The experiments were carried out in a Plexiglas tank of a size of 30cm width x 7.5cm depth x 50cm height (see Figure 2a), where a removable and flexible PET sheet is placed at 25 cm height to separate two different layers of fluid and ensure an initially sharp interface. The upper part is filled up to 13.5 cm with a lighter suspension of water and particles, the lower part is filled with a denser sugar and water solution. The upper layer is strongly mixed before each experiment to ensure an initially uniform concentration. Experiments consist in removing the separation and analyzing the formation of fingers. Each experiment is filmed by a HD camera. A process of calibration has been carried out to correlate the different grey levels of a film image to different level of concentration.

After the removal of the separation, if we consider the upper layer to behave as a simple quiescent suspension, we could expect its mean concentration to decrease linearly with time as follows:

$$C(t) = C_0 - \frac{C_0 w_s t}{h}$$

Preliminary observations showed us that this is not the case for our experiments (see Figure 2b). As a matter of fact, the concentration values start decreasing after a certain time following the opening of the separation. This could be due to the fact that the linear model does not take into account the accumulation of particles at the interface between the two layers at different densities, which actually causes gravitational instabilities. These first considerations confirm the fact that convective instabilities influence the rate of sedimentation and consequently underline the need to develop new and complete analytical expressions to improve modelling of sedimentation from buoyant plumes.

Figure 1: Examples of fingering generated at the base of horizontally-spreading volcanic clouds (Eruption of Montserrat, 1997. Photo by Costanza Bonadonna).

(a)

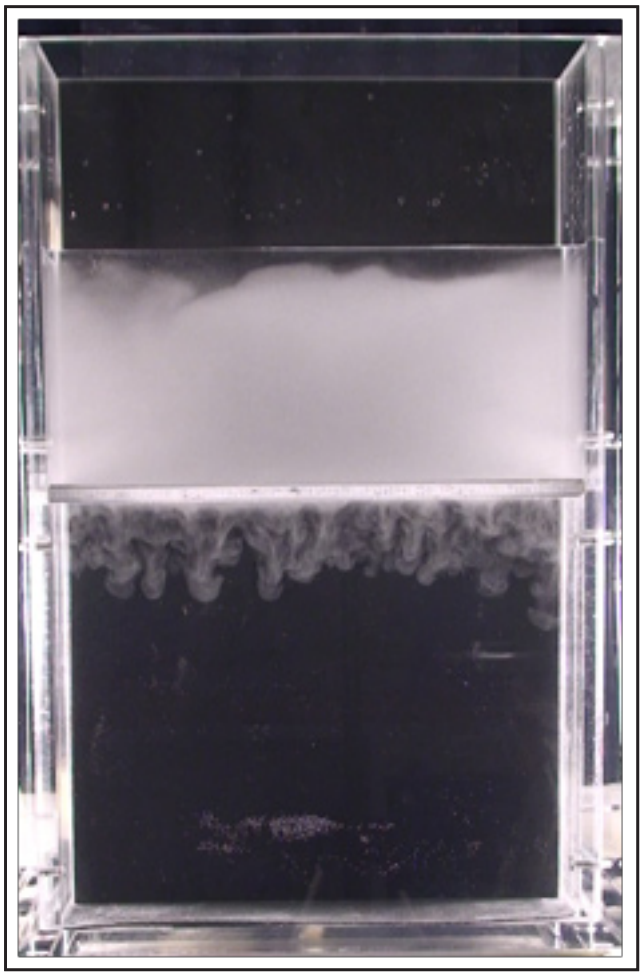

(b)

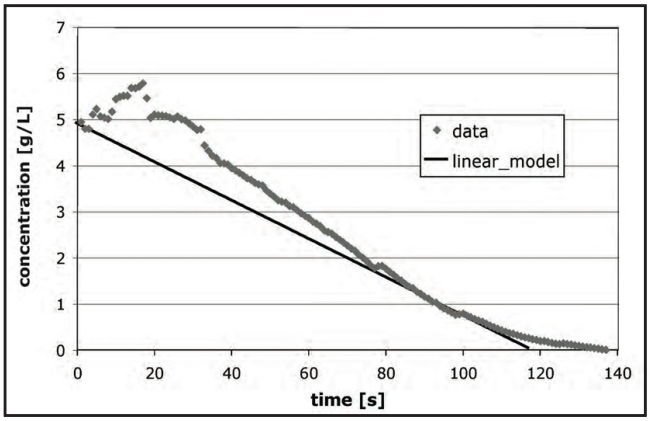

Figure 2: (a) The experimental set-up, a Plexiglas tank of 30x7.5x50 cm after the banner is removed. (b) Mean concentration for the upper layer as a function of time for an initial concentration of 4.9 g/L compared with the linear model.

REFERENCES

Carey, S. N. 1997: Influence of convective sedimentation on the formation of widespread tephra fall layers in the deep sea. Geology, 25(9), 839-842.

Chen, C. F. 1997: Particle flux through sediment fingers, Deep Sea Research Part I. Oceanographic Research Papers, 44(9-10), 1645-1654.

Hoyal, D. C. J. D., et al. 1999: Settling-driven convection: A mechanism of sedimentation from stratified fluids. J. Geophys. Res., 104.

Voltz, C., et al. 2000: Finger-like patterns in sedimenting water-sand suspensions. Physics Reports, 337, 117-138.

3.26

Geochemical constraints on the development of a Mesozoic volcano-tectonic arc and fore-arc basin in the Sanandaj-Sirjan Zone, south Iran

Monsef Iman*, Rahgoshay Mohammad*, Emami Mohammad-Hashem** & Shafaii Moghadam Hadi***

*Shahid Beheshti University, Faculty of Earth Sciences, Tehran, Iran (iman_monsef@yahoo.com)
**Research Institue for Earth Sciences, Geological Survey of Iran, Teharn, Iran
***Damghan University of Basic Sciences, School of Earth Sciences, Damghan, Iran

The tectonic history of the Neo-Tethyan region in Iran was begun by the creation of the oceanic lithosphere with rifting between the Central Iranian Block and Gondwana (Arabia) during Late Permian-Early Triassic time. The subduction of the Neo-Tethys starts to the south of the Central Iranian Block at Late Triassic–Late Jurassic time. This subduction phase led to presence of volcanic activities and emplacement of intrusive bodies within the Sanandaj-Sirjan Zone (Fig. 1). Therefore the Sanandaj-Sirjan Zone behaved as an active continental margin, witness by the presence of calc-alkaline arc-related magmatism. The Sanandaj-Sirjan Magmatic Arc is composed mainly of a Mesozoic magmatism including lava (basalt, andesite and dacitic tuff) and plutonic rocks (granite, granodiorite and quartz monzonite), alternating with limestones and Orbitolina limestone.

About a same time during subduction of the Neo-Tethys, rifting along the Sanandaj-Sirjan Zone took place, resulting in opening of a Late Triassic to Early Jurassic transtensional fore–arc basin called the Hajiabad–Esfandagheh Color Melange Zone (Fig. 1). This zone contains abundant ultramafics with chromite deposits, partly preserved volcano–sedimentary sequences with pillow lavas, Globotruncana–bearing red marls and radiolarites, and exotic marbles, amphibolites and minor blueschists. Volcanic rocks have a mixture of dominantly arc-like (calc-alkaline) and subordinate MORB-like compositional features.

The emplacement of Color Melange Zone took place during the Early to Late Cretaceous as a result of collisional and continental subduction of the Gondwana (Arabia) beneath the Central Iranian Block along the Main Zagros Thrust Belt. The Zagros orogen is a young Tertiary collision belt generally considered a recent analogue of the Himalayan orogenic belt.

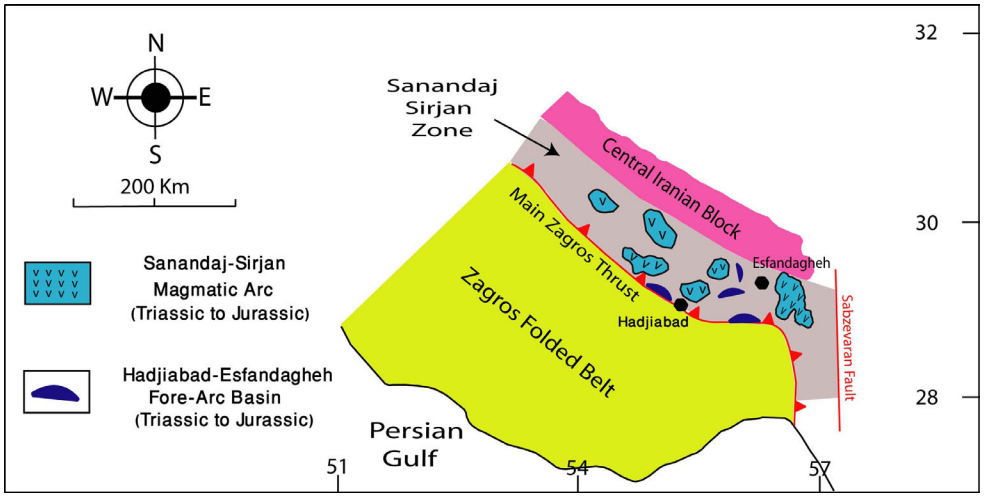

Figure 1. Simplified structural sketch map of south Iran. The locations of major structural zones consisting of Sanandaj-Sirjan Zone, Central Iranian Block, Main Zagros Thrust and Zagros Folded Belt are indicated.

REFERENCES

Agard, P., Monie, P., Gerber, W., Omrani, J., Molinaro, M., Meyer, B., Labrousse, L., Vrielynck, B., Jolivet, L. & Yamato, P., 2006: Transient, synobduction exhumation of Zagros blueschists inferred from P-T, deformation, time, and kinematic constraints: Implications for Neotethyan wedge dynamics. Journal of Geophysical Research, 111, B11401, 1-28.

Ewart, A., Collerson, K.D., Regelous, M., Wendt, J.I. & Niu, Y., 1998: Geochemical evolution within the Tonga-Kermadec-Lau arc-back arc systems: the role of varying mantle wedge composition in space and time. Journal of Petrology, 39, 331-368.

McCulloch, M.T. & Gamble, J.A., 1991: Geochemical and geodynamical constraints on subduction zone magmatism. Earth and Planetary Science Letters, 102, 358-375.

Pearce, J.A., 1980: Geochemical evidence for the genesis and eruptive setting of lavas from Tethyan ophiolites. In: Panayiotou, A., (Eds.), Ophiolites. Procceding International Ophiolite Symposium, Nicosia, Geological Survey Department, 261-272.

3.27

Transtensional basin system in Central Iranian Volcanic Belt

R. Monsef *, M.H. Emami**, N. Rashidnejad Omran***

* ISLAMIC AZAD UNIVERSITY,ESTAHBAN BRANCH,IRAN (zaos13000@yahoo.com)
**RESEARCH INSTITUE FOR EARTH SCIENCES, GEOLOGICAL SURVEY OF IRAN.
*** GEOLOGY DEPARTMANT BASIC SCIENCE FACULTY, TARBIAT MODARES UNIVERSITY,PO. 14115-111,TEHRAN

Urumieh-Dokhtar magmatic zone (UDMZ) has been considered as a place for the main magmatic activities in the Central Iranian continent in the Cenozoic(mainly in eocene).Magmatism is spatially and temporally associated with Alpine-Himalaya collisional tectonics. Explosive activities in Paleogene and early Neogene were commonly from fissure eruptions and feeder dikes had a domonant role for creation of thick sequences of magmatic and pyroclastic rocks. The Slafchegan to Delijan region covers an area about 500 sq. It is characterized by a number of sub parallel mountains and depressions, running NW-SE belongs to Neogene.centeral vent eruptions caused for creation of strata-volcanoes in the study area and varient of volcanic domes in continental environment. The Neogene volcanic activities are divided into two phases: At the first stage (Ngv_1), volcanic rocks contain basalt to andesite-basalt as lava or pyroclastic materials.The explosive event was followed by the volcanic to subvolcanic associations of Ngv_2 with products of mainly andesitic to rhyiolitic composition. The volcanic domes of Ngv_2 and their diverse modes of emplacement are especially characteristic of this phase as Kuh-e-Aleh (fig.1). Petrography,Geochemistry and mineral chemistry data confirm the presence of transtensional regions along the Urumieh-Dokhtar magmatic zone(UDMZ), opened during Paleogene and early Neogene due to the collision of the Arabia platform and Central Iranian continent. At Tertiary time, the time span between the Laramidian and Mio-Pliocene phase is related to the opening up of the basins (intercontinental rift), the extensional phenomenon moving slowly at the end of the Eocene and the beginning of the Oligocene. Local Nogene volcanism due to transtensional regions happens in Oligo-Miocene. The closing of the basins, or compressional period, began with the Mio- Pliocene movement which caused the folding and uplifting.

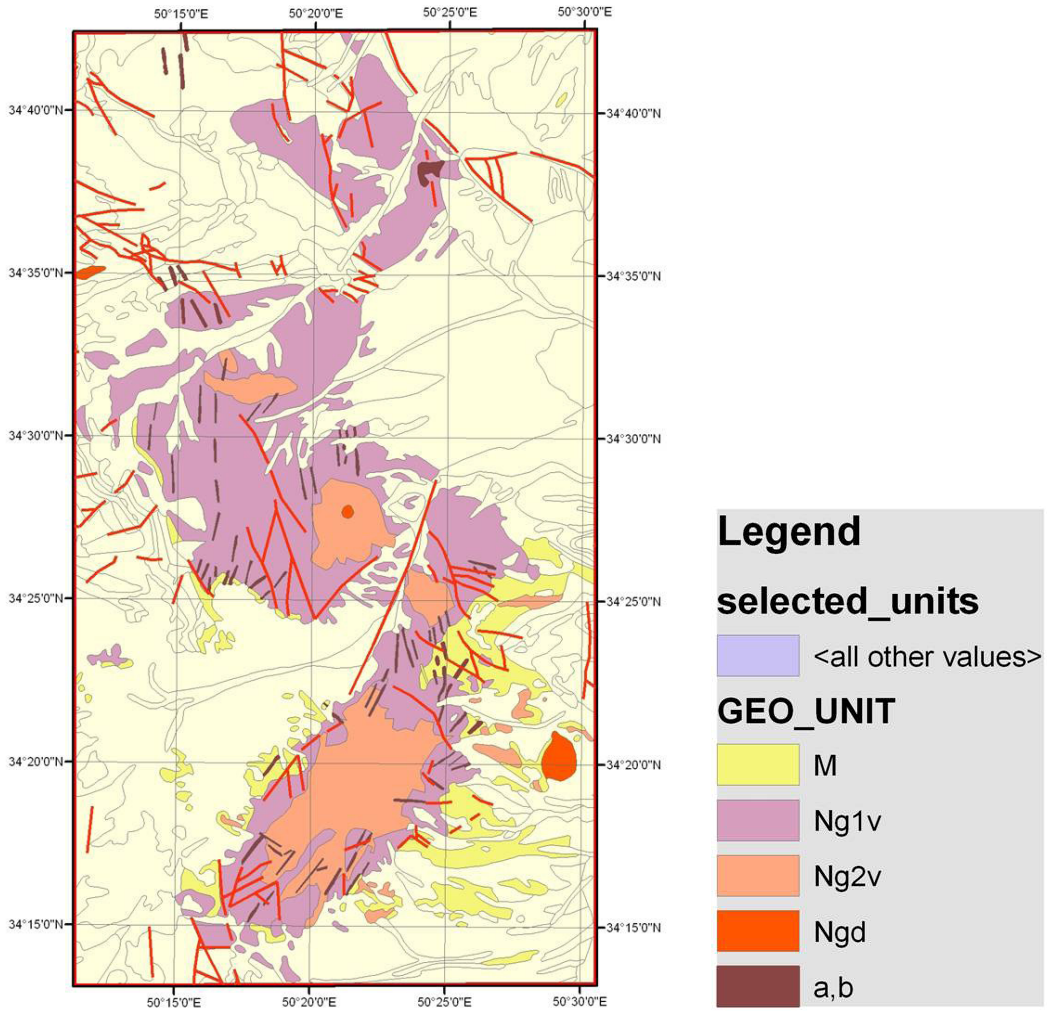

Figure 1. Geological our view map of Neogene volcanic activities.1:25000

REFERENCES
Emami. M.H., 1981, Geologie de la region de Qom-Aran (Iran) contribution a l etude dynamique et geochimique du volcanisme tertiaire de l Iran Central, These Doctorat Etat Grenoble, 489
Ricou, L.E., 1994. Tethys reconstructed plates, continental fragments and their boundaries since 260 Ma from Central America to South – eastern Asia. Geodynamica Acta (Paris) 7.
Verdel, Charles, 2009, Cenozoic Geology of Iran: An integretad study of extensional tectonics and related volcanism, Thesis doctor of philosophy,California Institute for Technology.

3.28

Metamorphic evolution of a kyanite-eclogite from Thermes, Rhodope Massif, Greece.

Moulas Evangelos*, Kostopoulos Dimitrios**

*Geologisches Institut, ETH Zürich, Sonnegstrasse 5, 8092 Zurich, Switzerland (moulase@student.ethz.ch)
**Department of Mineralogy and Petrology, Faculty of Geology and Geoenvironment, School of Sciences, National and Kapodistrian University of Athens, 157 84 Athens, Greece*

The Rhodope Massif in northern Greece is a recently identified ultrahigh-pressure metamorphic (UHPM) province comprising garnetiferous metapelites and eclogites with microdiamond inclusions. These rocks preserve evidence of melting (T>1100°C; P>7 GPa) in a Jurassic subduction zone and a complex reheating history at the base of the crust in the early Tertiary.

A kyanite-eclogite from the Thermes area reveals the pressure-temperature-time path followed by the Rhodope UHPM rocks. Textures involving phengitic mica indicate melting at high confining pressures. Quartz inclusions in kyanite show multi-polygonal domains and radial cracks suggesting former coesite, hence P conditions >2.7 GPa (at about 700°C).

Clinopyroxene formed under UHP conditions was replaced by diopside + plagioclase symplectites whereas kyanite was replaced by corundum + plagioclase symplectites during decompression. The latter reaction occurred in locally silica undersaturated domains of the rock (Godard & Mabit 1998). Large porphyroblastic amphiboles with taramitic cores mantled by pargasitic compositions attest amphibole formation via hydration reactions in the eclogite-facies and later decompression to the amphibolites facies.

Subsequent granulitisation proceeded via reactions between i) garnet porphyroblasts and matrix diopside to form coronas of plagioclase + ilmenite + magnetite + sodic gedrite around garnet, ii) corundum and diopside to form spinel + plagioclase symplectites after kyanite and iii) kyanite, spinel and corundum to form sapphirine (Liati & Seidel 1996). These imply that conditions of approximately 1.5 GPa at T>800°C were attained, possibly associated with a second-stage partial melting episode. Zircon geochronology using SHRIMP revealed a middle Eocene age (~42 Ma) for granulite formation. This age, in conjunction with the coeval age of apophyses of the Skaloti granite in the area, is consistent with the general history of the Rhodope Massif undergoing general exhumation and crustal collapse in Eocene times.

REFERENCES
Godard, G. & Mabit, J.-L. 1998: Peraluminus sapphirine formed during retrogression of a kyanite-bearing eclogite from Pays de Léon, Armorican Massif, France, Lithos 43, 15-29.
Liati, A. & Seidel, E. 1996: Metamorphic evolution and geochemistry of kyanite eclogites in central Rhodope, northern Greece, Contrib. Mineral. Petrol. 123, 293-307.

3.29

Rheological properties of crystal- and bubble-bearing silicic magmas: preliminary experimental results

Pistone Mattia *, Caricchi Luca **, Burlini Luigi ***, Ulmer Peter *

* *ETH-Institute for Mineralogy and Petrology, Clausiusstrasse 25, CH-8092 Zurich, Switzerland (mattia.pistone@erdw.ethz.ch; peter.ulmer@erdw.ethz.ch)*
** *University of Bristol, Wills Memorial Building - Queen's Road, BS8 1RJ Bristol (ca.luca@live.com)*
*** *ETH-Geological Institute, Sonneggstrasse 5, CH-8092 Zurich, Switzerland (luigi.burlini@erdw.ethz.ch)*

Natural magmas are mixtures of silicate melts, crystals and gas bubbles. The viscosity of such multi-phase mixtures is the single most important property controlling the eruptive behavior of volcanoes. The rheological behavior and the physical properties of magmas depend primarily on the viscosity of the silicate melt and on the relative contents of crystals and bubbles (Caricchi et al. 2007; Llewellin & Manga 2005) as well as on the interactions between these three phases.
The shape and size distribution of crystals has been demonstrated to influence significantly the variation of viscosity with respect to the crystal fraction. In addition, the non-Newtonian behavior of magmas (viscosity decreases with increasing deformation rate) has been associated to the geometrical ordering of suspended particles in the magma (Caricchi et al. 2007; Costa et al. 2009).

Bubbles exert contrasting effects on the rheological behavior of magmas depending on applied stress conditions. Deforming bubbles cause the viscosity to decrease while spherical gas vesicles behave as crystals, thus increasing the magma viscosity.
We present novel experimental results on the rheological behavior of magmas composed of liquid and both, gas-pressurized bubbles and crystals, deformed at magmatic pressures and temperatures. This study aims to constrain the dependence of rheological and physical properties of magmas on the viscosity of the silicate melt, on the relative contents of crystals and bubbles and on the interactions between these three phases.
The starting material constitutes of a haplogranitic melt containing variable amounts of H_2O (2.68 wt% and 5.25 wt%) and CO_2 (2.06 wt% and 4.97 wt%) and different proportions of quartz crystals (between 24 and 65 vol%; 63-125 μm in diameter) and bubbles (between 7 and 22 vol%; 5-150 μm in diameter).
The experiments were performed in simple shear using a HT-HP internally-heated Paterson-type rock deformation apparatus (Paterson & Olgaard, 2000) at strain rates ranging between $5{\cdot}10^{-5}$ s^{-1} and $1{\cdot}10^{-3}$ s^{-1}, at a pressure of 200 MPa and temperatures between 773 and 923 K.

At these temperature and strain rate conditions the silicate melt behaves as a Newtonian liquid (Webb & Dingwell, 1990). Consequently, non-Newtonian effects can entirely be related to the presence of bubbles and crystals. In all experimental runs a marked weakening behavior (decrease of stress with increasing strain) was observed.
Back-scattered electron images were acquired on external portions of the samples, where the simple shear configuration is best appreciated. These images clearly highlight the presence of melt-enriched portions of the samples were bubbles are strongly deformed. In contrast, in regions surrounding these melt-enriched bands, bubbles are almost spherical testifying that these portions of the material suffered a significantly lower amount of deformation. Locally, deformed bubbles between crystals resulting from local stress concentration generated by the solid particles can be observed. The measured weakening is most probably related to the generation of melt-enriched shear bands. The localization of deformation in these lower viscosity regions results in a decrease of viscosity with increasing strain (shear thinning effects).

These preliminary experimental results serve to guide our ongoing experimental efforts to finally obtain rheological laws for crystal and bubble bearing magmas to simulate and predict volcanic eruptions from shallow magma reservoirs and volcanic conduits.

REFERENCES

Caricchi, L., Burlini, L., Ulmer, P., Gerya, T., Vassalli, M. & Papale, P. 2007: Non-Newtonian rheology of crystal-bearing magmas and implications for magma ascent dynamics. Earth Planet. Sci. Lett. 264, 402-419.

Costa, A., Caricchi, L. & Bagdassarov, N.S. 2009: A model for the rheology of particle-bearing suspensions and partially molten rocks. Geochem. Geophys. Geosyst. 10, 1-13.

Llewellin, E.W. & Manga, A. 2005: Bubble suspension rheology and implications for conduit flow. J. Volcanol. Geotherm. Res. 143, 205–217.

Paterson, M.S. & Olgaard, D.L. 2000: Rock deformation tests to large shear strains in torsion. J. Struct. Geol. 22, 1341-1358.

Webb, S.L. & Dingwell D.B. 1990: Non-Newtonian rheology of igneous melts at high stresses and strain rates: experimental results for rhyolite, andesite, basalt and nephelinite. J. Geophys. Res. 95 (B10), 15695-15701.

3.30

Complexities in the high pressure metamorphic history of the central Sesia Zone near Cima di Bonze (NW Italy)

Daniele Regis*, Paola Manzotti*, Katherine Boston**, Benedicte Cenki-Tok*, Martin Robyr*, Daniela Rubatto**, Tonny Thomsen*, Martin Engi*

*University of Bern, Baltzerstrasse 3, CH-3012 Bern, Switzerland (regis@geo.unibe.ch)
**The Australian National University, Mills road, Canberra, ACT, 0200 Australia

The central Sesia-Lanzo Zone includes a narrow, continuously surfacing unit, which was termed Monometamorphic Cover Complex (MCC) by Venturini (1995). The MCC comprises: (a) the *Bonze Unit*, composed of basic rocks (metagabbros and glaucophane-eclogites), found in tectonic contact with (b) metasediments (calcschists, metamarls, impure quartzites) of the *Scalaro Unit*. The contacts between this body and the two large basement blocks of the Sesia Zone are clearly tectonic and mostly predate the eclogitic metamorphism.

Rubatto et al. (1999) showed that gabbros of the Bonze Unit had intruded the crystalline basement in the early Carboniferous. Blasto-mylonitic metagabbros contain local relics of brown hornblende; these may reflect pre-Alpine metamorphism (amphibolite facies?). However, no relics of a pre-Alpine stage have been found in the metasediments of the Scalaro Unit. This unit is thus a good target for structurally controlled petrochronology of the Alpine evolution in the central Sesia Zone.

We report results of detailed structural, petrographic, chemical and geochronological work carried out in the Cima Bonze region, with a focus on impure quartzites of the poly-deformed Scalaro Unit. A pervasive HP planar structure (S2 foliation) dominates in the area studied and in the samples analysed. Several generations of metamorphic allanite and LREE-rich epidote occur, providing a robust (Th-Pb, U-Pb) chronometer that can be intimately linked to the petrological and micro-structural evolution. Three growth zones with variable REE and U-Th contents were recognized in these allanites, and retrogressive tiny rims of clinozoisite/epidote were often observed. Phase relations between allanite and other REE-rich phases were carefully studied and yield a very clear and interesting sequence. Epidote often includes relics of monazite, thorite, apatite and xenotime. The phase relations indicate the reaction: monazite + fluid à allanite + thorite + apatite. Large crystals of xenotime forming coronas on zircon are associated with small crystals of thorite and REE-poor allanite.

SHRIMP U-Th-Pb *in situ* dating of the three growth zones consistently yield three different Alpine ages (from 83 Ma to 65 Ma). Preliminary LA-ICP-MS data on the same samples confirm the ion probe results. Further electron microprobe dating is underway on monazite and thorite to understand their relations to allanite and to unravel whether the early monazite is a prograde or a detrital phase.

These results have important implications on the Alpine HP-evolution of the Sesia Zone as a whole. A detailed PTDt-path is presently being be worked out, but the preliminary data in any case indicate a complex, protracted reaction sequence producing allanite over at least 10 m.y. This may serve to explain at least some of the complex Ar-Ar age patterns found by Venturini (1995).

REFERENCES

Rubatto D., Gebauer D., Compagnoni R. 1999: Dating of eclogite-facies zircons: the age of Alpine metamorphism in the Sesia-Lanzo Zone (Western Alps). Earth Planet. Sci. Letters 167, 141-158.

Venturini G. 1995: Geology, geochemistry and geochronology of the inner central Sesia Zone (Western Alps – Italy). Mémoires de Géologie, Lausanne, 25, 148 pp.

3.31

The temporal evolution of the Mitu group, south-east Peru – first U-Pb age data.

Reitsma Mariël*, Schaltegger Urs*, Spikings Richard*, Carlotto Victor**

*Earth and Environmental Sciences, Rue des Maraîchers 13, CH-1205 Genève
**INGEMMET, Av. Canada 1470 San Borja, Lima, Peru

The Eastern Cordillera of southern Peru formed along a crustal zone that has been active as part of the western Gondwana margin since the middle Paleozoic. The present study investigates the Mitu Group of south-east Peru in the area of Abancay-Cusco-Sicuani-Titicaca. This unit comprises continental clastic sediments deposited in syn-sedimentary basins during an extensional period in Permo-Triassic times and has not benefitted from a thorough geochemical-geochronological investigation so far. One of the main reasons for this lack of data is a complex structure of the graben system, tectonically complicated by compressional inversion of the extensional basins during Andean orogeny. Due to dominating coarse-grained clastics, the Mitu Group is devoid of fossils and its age is only poorly bracketed to be Permo -Triassic based on its stratigraphic relation to the underlying Copacabana and overlying Pucara groups. The upper levels of the Copacabana have been constrained by palynology to the Artinskian (Doubinger and Marocco, 1981). However, a hiatus may be observed between the Copacabana and the Mitu groups in most places, rendering the age estimate of the basal Mitu imprecise. The Pucara Group, regarded by Rosas et al. (2007) as thermal sag after Mitu extension, is attributed to the late Triassic - early Jurassic on the basis of ammonite fossils and U-Pb zircon ages from ash beds (Schaltegger et al., 2008). The aim of this study is to provide more accurate and precise age constraints for the age and duration of the Mitu Group by using U-Pb geochronology of volcanic zircon in rhyolitic lavas, and of detrital zircon in clastic sediments. For andesitic volcanic lithologies, age approximations will be obtained by Ar-Ar techniques applied to amphibole and groundmass samples.

Field data were obtained from a long and apparently complete section through the Mitu, situated 120km SE of Cusco near the city of Sicuani. This section consists of typical Mitu deposits; continental red beds, breccias and andesitic lavas. However, a zircon-bearing rhyolitic lava at the bottom gives us the opportunity to date the start of Mitu sedimentation by U-Pb ID-TIMS; this analysis will provide a precise age for the base of the Mitu group for the first time. In the Sicuani area the Mitu unconformably overlies the Ambo group, suggesting that the entire Copacabana is missing. Laser-ablation ICP-MS U-Pb data of detrial zircons from a sandstone just below the unconformity indicate a maximum age of latest Carboniferous (303Ma) for the underlying Ambo group. This maximum age overlaps with the palynological age of the lower Copacabana (Azcuy et al., 2002), raising the question whether the Ambo and Copacabana are truly diachronous or just coeval units of different sedimentary facies associations.
In another section, 100km W of Cusco, near the city of Abancay, we found Mitu sediments overlying the Copacabana Group. Here the Copacabana contains well preserved plant fossils of the lycopsids family also found elsewhere in Peru and Bolivia. Lack of acidic volcanism during Mitu extension in this region prevents from dating of lavas using the U-Pb method. The detrital zircon population in a sandstone in the lowermost part of the Mitu was analysed for U-Pb ages, using LA-ICP-MS techniques. The youngest zircons in the population are around 235 Ma hence providing a maximum age for the onset of Mitu group sedimentation. The Artinskian age for the upper Copacabana from Doubinger and Marocco (1981) has also been obtained from the Abancay region, establishing a hiatus of some 50 Myrs between the two units. The Mitu Group is intruded by a 220 Ma granite body (Lipa and Saraiva, 2008) indicating significant burial of the sediments at this time.
500km SE of Cusco, on the Bolivian shores of lake Titicaca, the Ambo Group features plant fossils of the Lycopsids family like those found in the Copacabana near Abancay. Our detrital zircon LA-ICPMS study on a quartz arenite just below the fossils indicates a maximum U-Pb age of 343Ma. However a zircon-bearing ash bed will allow for more precise calibration of the fossil age by ID-TIMS techniques. The zircon U-Pb data will provide a test whether the Copacabana and the Ambo group are indeed diachronous or just lateral variations of a sedimentary system.

REFERENCES

Azcuy, C.L., Di Pasquo, M. & Valdivia Ampuero, H. 2002: Late Carboniferous miospores from the Tarma Formation, Pongo de Mainique, Peru. Review of palaeobotany and palynology 118, 1-28.

Doubinger, J., and Marocco, R. 1981 : Contenu Palynologique du Groupe Copacabana (Permien Inférieur et Moyen) sur la bordure Sud de la Cordillère de Vilcabamba, région de Cuzco (Pérou). International Journal of Earth Sciences 70, 1086-1099.

Lipa Salas, V. & Saraiva Dos Santos, T. 2008: Geocronologia y evolucion tectonica del pluton Abancay-Apurimac-Peru. XIII Latin-American geological congress: Lima, Peru.

Rosas, S., Fontboté, L. & Tankard, A. 2007: Tectonic evolution and paleogeography of the Mesozoic Pucara Basin, central Peru. Journal of South American Earth Sciences 24, 1-24.

Schaltegger, U., Guex, J., Bartolini, A., Schoene, B. & Ovtcharova, M. 2008: Precise U-Pb age constraints for end-Triassic mass extinction, its correlation to volcanism and Hettangian post-extension recovery. Earth and Planetary science letters 267, 266-275.

3.32

Single-crystal elastic properties of superhydrous phase B determined by Brillouin scattering spectroscopy

Rosa Angelika D.*, Sanchez-Valle Carmen*, Wang Jingyun* & Saikia Ashima*

Institute for Mineralogy and Petrology, ETH Zurich, Zurich 8092, Switzerland (angelika.rosa@erdw.ethz.ch)

Superhydrous phase B, $Mg_{10}Si_3O_{18}H_4$, (here referred to as ShyB) belongs to the group of DHMS phases (dense hydrous magnesium silicates), that are likely the most important water reservoirs in deep subducted slabs.
In order to formulate accurate mineralogical and compositional models of subducted slabs and to interpret seismic observation in this area, precisely measured elasticity data at relevant P-T conditions are needed but are not often available.

In this contribution we present results of Brillouin scattering measurements of the sound velocities and single-crystal elastic properties of ShyB at ambient conditions. Brillouin scattering is one of the most powerful and precise method to investigate the elastic properties of single-crystals and polycrystalline samples of small size. The ShyB single-crystals used here were synthesised in a Walker module multi anvil press of 1000 ton at IMP, Zurich at 20 GPa and 1200 ^{0}C. The Voigt-Reuss-Hill average for the adiabatic bulk and shear moduli are Ks = 150(3) GPa and μ = 98(2) GPa, respectively. The present results are in good agreement with a previous Brillouin scattering study by Pacalo & Weidner (1996) [1]. The bulk modulus obtained in this study is also in good agreement with the results of a previous single-crystal PV study [2] but resolve discrepancies between previous compressional studies using powdered samples [3,4]. The results show that the aggregate compressional and shear wave velocities of ShyB (V_P = 9.17(9) and V_S = 5.43(4) km/s) are the lowest among coexisting phases in subducted peridoties, including Mg-Perovskite, hydrous Ringwoodite or Ferropericlase. The velocity distribution calculated from the best-fit elastic model of ShyB reveals a nearly isotropic seismic behaviour of ShyB at room conditions. The compressional anisotropy (A_P) is only 6.6% while slightly higher shear anisotropy (A_S) of 11.6 % is observed. If the moderated anisotropy of ShyB is maintained at high P-T, the strong seismic anisotropy observed in subducted slabs below the transition zone, may not be related to the presence of ShyB.

REFERENCES

[1] Pacalo, R.E.G. and Weidner, D.J. 1996: Elasticity of superhydrous B. Physics and Chemistry of Minerals, 23, 520-525.
[2] Kudoh, Y., Nagase, T., Ohta, S., Sasaki, S., Kanzaki, M., and Tanaka, M. 1994: Crystal structure and compressibility of superhydrous phase B, Mg20Si6H8O36. In S.C. Schmidt, J.W. Shaner, G.A. Samara, and M. Ross, Eds. High-Pressure Science and Technology, Am. Inst. Phys. Conf. Proc., 309, p. 469-472.
[3] Inoue, T., Higo, Y., Yamada, A., Irifune, T. &Funakoshi, K. 2006: High-pressure and high-temperature stability and equation of state of superhydrous phase B by insitu X-ray diffraction. In S.D. Jacobsen, and S. Van der Lee, Eds. Earth Deep Water Cycle, p. 147-157. AGU, Washington DC.
[4] Litasov, K.D., Ohtani, E., Ghosh, S., Nishihara, Y., Suzuki, A. and Funakoshi, K. 2007: Thermal equation of state of superhydrous phase B to 27 GPa and 1373 K. Physics of the Earth and Planetary Interiors, 164, 142-160.

3.33

The influence of volatiles in basaltic explosive eruptions: the example of the Chaimilla eruption (3.1 Ka, Villarrica Volcano, Chile).

Scalisi Rosalinda1, Costantini Licia1, Bonadonna Costanza1, Di Muro Andrea2

1Section des sciences de la Terre et de l'environnement 13, Rue des Maraichers, Ch-1025 Genève (s.linda84@tiscali.it)
2Laboratoire de physique et chimie des systèmes volcaniques, IPGP-Paris VI, Paris, France

Villarrica is a basaltic-andesite stratovolcano located in the Southern Chilean Andes. It is one of the most active volcanoes in South America associated with east-dipping subduction of the Nazca plate beneath the South American plate. Although its historical eruptive activity has been mainly effusive, in its history Villarrica volcano had also explosive behavior producing both large pyroclastic density currents and tephra fallout. The largest-volume eruptions are the Lìcan Ignimbrite (~10Km^3, ~14,000 BP) and Pùcon Ignimbrite (~5Km^3, ~3500BP) (Witter et al., 2004), both of basaltic-andesite composition. The most re-

cent pyroclastic density current occurred ~1620 BP (Moreno et al., 1994). After the last eruption (1984-1985), Villarrica volcano has had a continuous passive degassing activity from the summit lava lake (Witter et al., 2004).
In this project we have investigated the initial condition of Villarrica magma storage reservoir and the role of different volatile species in controlling the eruption dynamics of Chaimilla deposit (~3,100 BP), which is the best preserved and most widely dispersed tephra fallout of Villarrica volcano. This is done by a detailed petrographical and geochemical study of olivine-hosted melt inclusions and of all the phases present in the system (i.e. minerals and glass matrix).

The petrographical and geochemical study has been carried out at the University of Geneva and Lausanne (for EMP analysis) with the exception of H_2O and CO_2 analyses of melt inclusions which was done at the Laboratory Pierre Sùe (Paris, France) using both FTIR and RAMAN techniques.

Our preliminary results show that the magma chemistry did not change during the evolution of the eruption (SiO_2 content of whole rock is ~53 wt% and SiO_2 content of melt inclusion varies between 52 and 56 wt%) with exception of the uppermost fallout layers, which show a slightly more primitive composition (SiO_2 content of whole rock is ~52 wt% and SiO_2 content of melt inclusion is ~51 wt%). Pre-eruptive H_2O content is relatively high (~2-3 wt%) for a basaltic magma, but this high content has been frequently found in other high-explosive basaltic eruptions (e.g. Metrich et al.,2004; Spilliaert et al., 2006; Roggensack et al., 1997). In addition Chaimilla melt inclusions do not contain CO_2 suggesting a relatively shallow magma reservoir.

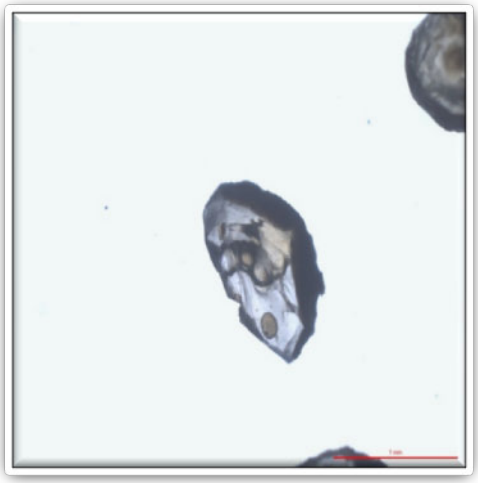

A

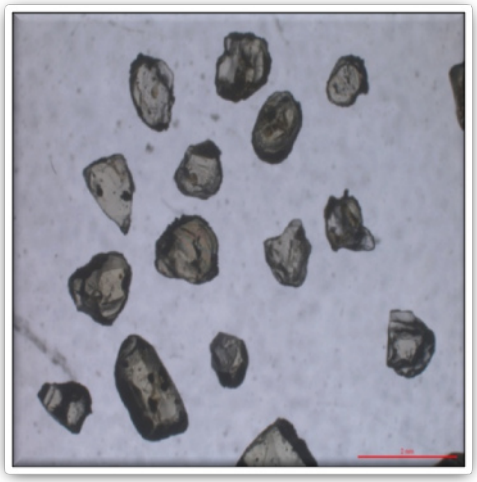

B

Fig A: melt inclusion present in olivine (Samples from Chaimilla scorias, Villarrica volcano, Chile). Fig B: different olivine crystals of Chaimilla deposit.

REFERENCES

Métrich N, Allard A, Spilliaert A, Andronico D, Burton M (2004). 2001 flank eruption of the alkali- -and volatile-rich primitive basalt responsible for Mount Etna. Earth and Planetary Science Letters, 228, 1-17.

Moreno H, Clavero J, Lara L. (1994). Actividad explosiva post-glacial del volcano Villarrica , Andes del Sur. Septimo congreso geologico chileno. Universidad de concepcion. Conception, Chile, 329-333.

Roggensack K, Hervig RL, McKnight SB, Williams SN (1997). Explosive basaltic volcanism from Cerro Negro volcano: Influence of volatiles on eruptive style. Science, 277, 1639-1642.

Spilliaert N, Allard P, Metrich N, Sobolev AV (2006). Melt inclusion record of the conditions of ascent, degassing and extrusion of volatile-rich alkali basalt during the powerful 2002 flank eruption of Mount Etna (Italy). Journal of Geophysical Research 111:doi: 10.1029/2005JB003934.

Witter J.B, Kress V.C, Delmelle P, Stix J (2004). Volatile degassing, petrology, and magma dynamics of the Villarrica Lava Lake, Southern Chile. Journal of Volcanology and Geothermal Research, 134, 303-337.

3.34

An experimental study in the system Fe-Mg-Ti-Cr-Si-O±Al: ilmenite solid solution as a function of pressure and temperature

Semytkivska Nina*, Ulmer Peter*

Department of Earth Science. ETH Zurich, Clausiusstr.25, 8092 Zurich

With the aim of improving the experimental basis of the calibration in the system Mg-Fe-Ti-Cr-Al-Si-O, we done experimental study with particular attention to picro-ilmenite.
Experiments were performed at temperature of 1000-1400 ^{o}C and pressure of 2.5, 3.5, and 5 GPa using different bulk compositions with variable Mg/Fe, Cr/Al ratios, and silica activity under relatively reducing conditions by employing graphite containers sealed into Pt-capsule. Experiments were run in solid-media piston cylinders and multi-anvil apparatus for durations of 30-120 hours.
Different phase paragenesis was observed at our experimental products. Bulk composition has a marked effect on the phase paragenesis, in particular, stability of the phases is influenced by the Mg# of the system. Ilmenite is stable together with olivine + orthopyroxene + spinel at bulk XMg of 0.73 (tab. 1, 2). rutile + olivine + opx + spinel are coexisting phases at a bulk X_{Mg} of 0.85 . Composition with lower SiO2 contents and low XMg values are characterized by the presence of three oxides: ilmenite + rutile + spinel coexisting with olivine and opx. Compositions with high X_{Mg} (0.85) and lower SiO_2 contents result in the disappearance of opx and rutile; present phases are olivine + spinel + ilmenite.

The experimental data set was used to determine equilibrium fractionation of Fe and Mg between coexisting ol and ilm, and applied to formulate model for ilmenite solid solution and intended to provide a new version of ilmenite-olivine an exchange geothermometer that could be applicable to the Cr-rich assemblage.

3.35

Pyroxenite veins in the Jurassic Pindos Ophiolite (NW Greece): cm-scale mantle heterogeneity preserved in MORB-source peridotites

Dmitry S. Sergeev*,**, Arjan H. Dijkstra*

*Université de Neuchâtel, Institut de Géologie et d'Hydrogéologie, Switzerland (dmitry.sergeev@unine.ch)
**Université de Lausanne, Institut de Minéralogie et Géochimie, Switzerland*

Geochemical and isotopic differences between different types of MORB are commonly attributed to heterogeneity in the mantle source. One of the major factors that can cause such heterogeneity is the presence of recycled ocean crust. We believe that traces of such heterogeneities can be preserved in pyroxenite veins in ophiolitic peridotite bodies. The Dramala Complex in the Pindos ophiolite (NW Greece) is a peridotite body with a mid-ocean ridge character, where we found a km-sized structural domain with coarse-grained mantle tectonites and 1-10 cm thick pyroxenite veins. Pyroxenites are concordant to the high temperature deformation structures in the host peridotites and show metamorphic, replacive textures in thin sections.

We measured Highly Siderophile Elements (HSE, i.e., Os, Ir, Ru, Pt, Pd, Re) and Os isotope ratios in whole rock pyroxenites and wall-rock peridotites. Pyroxenites were carefully cut from the enclosing peridotites. HSE patterns in both cases have identical character; some small differences in incompatible HSE concentrations (Pt, Pd, Re) occur due to the presence of sulphides in pyroxenites. Peridotites have chondritic to subchondritic $^{187}Os/^{188}Os$ ratios (0.1196-0.1291), whereas the pyroxenites are all significantly more radiogenic ($^{187}Os/^{188}Os$=0.1418-0.1980). These difference cannot simply be explained by differences in Re/Os ratios between peridotites and pyroxenites. Geochemical and petrographic data show that concordant pyroxenites represents relics of replacive pyroxenites formed melt-rock reaction between pyroxene-saturated melts and peridotite.

The fact that pyroxenite layers are parallel to the foliation in high-temperature deformed peridotite tells us about their early-stage origin. Based on textures and HSE concentrations, we propose that pyroxenites exposed now are replacive products

of SiO_2-rich melts, derived from the melting of old mafic layers within the peridotites, with very radiogenic $^{187}Os/^{188}Os$ isotope ratios, since no other source of high $^{187}Os/^{188}Os$ isotope ratio is likely to exist in these rocks. Moreover we suggest that the melt did not generally migrate over large distances perpendicular to the pyroxenites, i.e., that the pyroxenites are essentially the wall-rock of the old mafic layers. If our interpretation is correct, then these are the first traces of isotopic mantle heterogeneity in residual MORB-source mantle observed so far. The presence of pyroxenites with superchondritic Os isotope ratios in the mantle can explain why estimates for $^{187}Os/^{188}Os$ isotope ratios of depleted mantle rocks are generally subchondritic.

3.36

The Zagros Collision Zone: Petrological and geodynamical constraints on Inner and Outer Zagros Ophiolitic Belt

Hadi Shafaii Moghadam *, Robert J. Stern **, Mohamad Rahgoshay ***

*School of Earth Sciences, Damghan University of Basic Sciences, Damghan, Iran, E-mail: hshafaii@dubs.ac.ir
** Geosciences Department, University of Texas at Dallas, Richardson, TX 75083-0688, USA
***Faculty of Earth Sciences, Shahid Beheshti University, Tehran, Iran

Despite broad affinities to other ophiolites in the Tethyan Mediterranean-Oman ophiolite belt, the upper Cretaceous ophiolites of SW Iran remain relatively unknown in terms of geochemistry, petrogenesis and tectono-magmatic evolution. Zagros ophiolites comprise two parallel belts, including Inner Zagros Ophiolitic Belt (IB), along the SW periphery of the Central Iranian block and Outer Zagros Ophiolitic Belt (OB), south of Main Zagros Thrust Fault. IB and OB ophiolites formed at the same time: IB hornblende gabbros yield a K/Ar age of 93 Ma whereas OB diabases and hornblende gabbros yield Ar/Ar ages of 86-93 Ma, similar to ages of other ophiolites of the Mediterranean-Oman belt (Oman ~95 Ma, Cyprus ~90-94Ma). Pelagic limestones resting conformably on IB and OB ophiolites are Turonian-Maastrichtian (93.5-65.5 Ma). Several lines of evidence such as high Cr content of harzburgite spinel and flat REE patterns of the lavas with negative Nb-Ta anomalies from both inner and outer belt Zagros ophiolites indicate formation above a subduction zone, also similar to other Tethyan Oman-Mediterranean ophiolites. These similarities in ophiolite ages and tectonic setting suggest that the Oman-Mediterranean ophiolite belt represents a remarkably coherent lithospheric block. The parallel alignment of Zagros ophiolites between the Urumieh-Dokhtar arc and the Zagros fold-and-thrust belt (accretionary prism), further suggests that IB and OB ophiolites may be exposed limbs of a deformed anticlinoria, and represent fore-arc basement. In this interpretation, IB and OB represent inner and outer portions of the Late Cretaceous Iranian fore-arc, developed over an incipient N-dipping subduction zone on the southern Eurasian margin. The Zagros fold-and-thrust best is an accretionary prism that formed by off-scraping of Arabian Plate sediments, and the Urumieh-Dokhtar arc is an Andean-type arc that is waning as the region transitions from subduction to collision.

3.37

The transition from cold-wet to hotter-drier rhyolites in subduction zones: the case of the Kos-Nisyros-Yali volcanic center, Aegean arc, Greece

Skopelitis Alexandra*, Bachmann Olivier**

*Earth and environmental science, Rue des Maraîchers 13, CH-1205 Genève, (Alexandra.Nowak@unige.ch)
**University of Washington, Earth and Space Sciences Seattle, WA 98195-1310 (bachmano.@u.washington.edu)

The complexity of magmatic chamber mechanisms are extensively studied but not completely understood. Several parameters, such as temperature, pressure, melt composition and cristallinity, can modify rheology, geochemistry, and geometry of the chamber and therefore have an important influence on the type and style of eruption. Magma viscosity is strongly linked with water content, crystal content and temperature.

Two kinds of rhyolites have been defined in the literature (Christiansen 2005): the first kind is cold (<750 °C) and oxidized (NNO+1) whereas the second kind is hotter (≥850 °C) and more reduced (~NNO or lower). Although both are at or near volatile saturation in shallow crustal magma chambers, the cold-oxidized type is obviously more water-rich, as it contains biotite and lacks pyroxene. The wet type is usually found in subduction zone settings, whereas the drier type is more characteristic of hot spot and extensional environments where mantle melting occurs by adiabatic decompression.

The present study shows that both types of rhyolites can be found in the same locality in the Aegean Arc in Greece (Fig. 1). We compared rhyolitic pumices of the Kos Plateau Tuff (KPT eruption age: 160 ky, (Smith et al. 1996)) from Kos Island to Nisyros and Yali, two southernmost islands. The rocks chemistry shows evolved compositions with an average around 70 %wt SiO_2 for Nisyros and 75-76 %wt SiO_2 for KPT and Yali.

The caldera-forming KPT erupted from a shallow (1.5-2.5 kb) near-solidus (~670-700 °C) and oxidized (NNO+1) magma chamber that was saturated with a water-rich gas phase. The following eruptions from Nisyros and Yali were in contrast, 100-150 °C hotter, less oxidized (~NNO) and mainly contained plagioclase and clinopyroxene (although Yali does contain minor quartz and sanidine as well). The reason for this shift from wet to drier rhyolites can be due to either (1) a change in parental basalt composition (drier basalts leading to drier rhyolites) or (2) an efficient degassing event induced by the caldera-forming event. More studies, including experiment work to reconstruct the temperature-pressure conditions before eruptions, are needed to better understand which scenario contributed to the observed shift in these rhyolites.

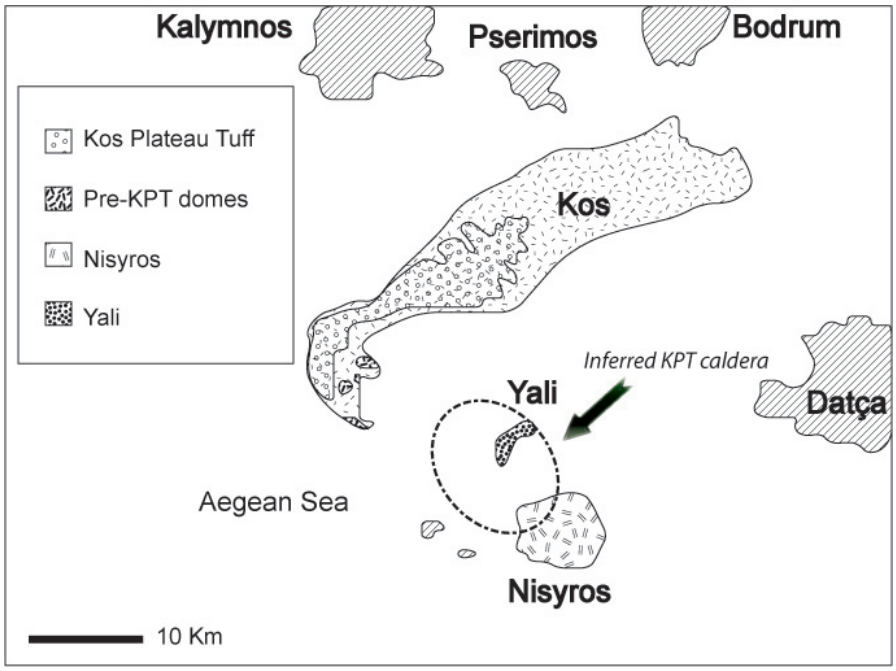

Figure 1. Simplified map of Kos, Nisyros and Yali. (Modified after Allen, 2001)

REFERENCES

Allen, S.R. 2001: Reconstruction of a major caldera-forming eruption from pyroclastic deposit characteristics: Kos Plateau Tuff, eastern Aegean Sea. Journal of Volcanology and Geothermal Research 105, 141-162.

Christiansen, E.-H. 2005: Contrasting processes in silicic magma chambers; evidence from very large volume ignimbrites. Geological Magazine 142(6), 669-981.

Seymour, K.S. & Lalonde, A. 1991: Monitoring oxygen fugacity conditions in pre, syn- and postcaldera magma chamber of Nisyros volcano, Aegean island arc, Greece. Journal of Volcanology and Geothermal Research 46, 231-240.

Smith, P. E., York, D., Chen, Y. & Evensen, N.M. 1996: Single crystal 40Ar/39Ar dating of a Late Quaternary paroxysm on Kos, Greece: Concordance of terrestrial and marine ages. Geophysical Research Letters 23, 3047-3050.

Volentik, A., Vanderkluysen, L., Principe, C. & Hunziker, J.C. 2005: Stratigraphy of Nisyros volcano (Greece). The geology, geochemistry and evolution of Nisyros Volcano (Greece). Implications for the volcanic hazards. Mémoires de Géologie (Lausanne), 26-66.

3.38

Dynamics of Cd, Pb and Cu cycling in a stream under contrasting photo-benthic biofilm activity and hydrological conditions

Tercier-Waeber Mary-Lou*, **, Hezard Teddy* & Masson Matthieu**

*CABE – Department of Inorganic, Analytical and Applied Chemistry, University of Geneva, Sciences II, 30 Quai E.-Ansermet, CH-1211 Geneva 4 (Marie-Louise.Tercier@unige.ch)
**Institut F.-A. Forel, University of Geneva, 10 Route de Suisse, CH-1290 Versoix

The past decade studies performed in rivers and streams demonstrated that many trace metal and metalloid experience diurnal cycles, with total dissolved metal concentrations often changing one- to five-fold during a 24h period. However, most of these studies were performed in summer under low-flow conditions. Moreover, samples were collected hourly by hand for later laboratory analysis. This laborious sample collection and processing approach limits hourly sampling to 1–3 days at maximum. More frequent analysis is required to understand the seasonal occurrence and amplitude of diel metal cycles, and the processes controlling these cycles.

With this goal in mind, we applied an automated voltammetric analyzer to study, at time scale of hour and under contrasting bio-chemical and hydrological conditions, the diurnal evolution of Cd, Cu and Pb in the Riou-Mort river (France) impacted by polymetallic pollution resulting from former open-cast coal mining and ore treatment. This analyzer is based on a bioanalogic microsensor which allows in situ real-time monitoring of the dynamic fraction, i.e. the potentially bioavailable fraction, of the target analytes. In parallel, T, pH, dissolved oxygen and conductivity were monitored in situ and water samples were collected for complementary analyses of the water composition.

Several original results were obtained. The data revealed that, in the studied river, the diurnal cycles of the Cd, Cu and Pb dynamic species were controlled by redox and sorption effects induced by either: pH diurnal cycle linked to metabolic activity of benthic biofilms; photoreduction of colloidal Mn oxides; and/or biofilm exudation of extracellular polymeric substances. We also observed that: the dynamic fraction of a given cationic metal can show diurnal cycle with opposite trends depending on the bio-chemical conditions; the trends of the diurnal dynamic metal species cycles may be different that those reported for the dissolved metal species. The importance of these findings will be discussed in the context of interpreting existing data banks, assessing metal ecotoxicity impact, and designing more appropriate monitoring control strategies.

REFERENCES

Tercier-Waeber, M.-L. & Taillefert, M. 2008: Remote in situ voltammetric techniques to characterize the biogeochemical cycling of trace metals in aquatic systems. J. Environ. Monit.,10, 30-54.

Tercier-Waeber, M.-L., Hezard, T., Masson, M., & Schäfer J. 2009: In situ monioring of the diurnal cycling of dynamic metal species in a stream under contrasting photobenthic biofilm activity and hydrological conditions, Env. Sci. Technol., DOI: 10.1021/es900247y.

3.39

LAMBERN – software for U-Pb, Th-Pb and Pb-Pb age dating by LA-ICP-MS analysis

Thomsen Tonny B.*, Pettke Thomas*, Allaz Julien*** & Engi Martin*

* University of Bern, Institute of Geological Sciences, Baltzerstrasse 1+3, CH-3012. (thomsen@geo.unibe.ch)
** University of Massachusetts Amherst, Department of Geosciences, 611 North Pleasant Street, USA

For U-Pb, Th-Pb and Pb-Pb age dating, the LA-ICP-MS offers a cost reducing and time efficient technique compared to e.g. TIMS and SIMS, by which a bulk of data with a moderate precision (typically <2 %) can be obtained in a very short time (e.g. 50-100 ages in 1-2 days). To compare the obtained data, standardized protocols accepted by the LA-ICP-MS age dating community and associated software able to handle and calculate ages from the various solid phases are required. At present, little soft-

ware is available (e.g. LAMTRACE, GLITTER, Lamdate, PEPITA, ComPbCorr, PbI; summarized in Ko ler & Sylvester, 2003 and Košler et al., 2008). Some of these assume no initial Pb present (LAMTRACE, GLITTER), however, some geologically relevant minerals such as allanite, titanite, rutile and perovskite may contain a significant proportion of common Pb. Other approaches rely on a nebulization-induced spike bracketing technique (Lamdate), an approach that is not employed in all laboratories.

Thus, we present here a transparent, step-by-step Excel-based data reduction procedure for in-situ solid state U-Th-Pb-based age determinations by LA-ICP-MS. The software (called LAMBERN) is able to handle all solid phases with sufficient U, Th and Pb content for age dating by LA-ICP-MS, including phases with a significant common Pb proportion. The software offers full control in all steps of the consecutive and flexible data reduction approach (includes several options for data correction and age calculation procedure). All data treatment, age calculation and error propagation are carried out in a single Excel file. Various diagrams, including time-intensity, time-ratio, sensitivity, ablation yield, Concordia, Tera-Wasserburg are generated. The output can be read directly by IsoPlotEx (Ludwig, 2003) for additional plotting and calculations.

LAMBERN employs a standard-sample-standard bracketing approach with a maximum of 20 individual analyses imported through an integrated VBA macro of xl, txt or csv files (from Elan, Thermo Finnigan Element2 or ThermoX). Time intervals for background and signal are selected by the user. Screening of the signals for extreme values (technically induced "outliers") and for signals of poor quality (e.g. from time-dependant fractionation) is carried out through time-intensity and time-ratio diagrams and includes an option for the rejection of data from a tolerated relative standard deviation ( ) specified by the user. The rejection of data includes entire sweeps.

Options for the data correction is specified in the setup parameters section and include background correction, mercury interference correction (of ^{204}Hg on ^{204}Pb), correction for instrumental mass bias (Linear, Power and Exponential Laws, Russell and Baxter formulations), detector drift and 3 different common Pb correction routines (measured 204 and the "207Pb" and "208Pb" corrections). Matrix effects calibration can be applied if required. Selection is done between (i) non-matched matrix based on e.g. NIST SRM-610 glass or (ii) matrix matching employing one or more (in-house) reference materials of known age (e.g. Harvard91500 zircon for analysis of zircons of unknown age).

At present, the robustness of the screening and calculation procedures in LAMBERN are being tested through analyses of standard zircons (91500zircon, Temora-1, Plesovice), allanites (AVC, CAP, Tara, Daibosatsu, Bona, Sissonne), titanite and monazite (in-house standards). In general, the accuracy of non-matrix matched calibration routines for zircon, allanite and in part titanite report up to 30% deviation from "true" ages (e.g. TIMS, SIMS). Thus, matrix-matched calibration is employed. At the time of reporting, LAMBERN has been in use by only a handful of test-users, thus is a "beta" version.

REFERENCES

Košler J., Forst L. & Sláma J. (2008) LamDate and LamTool: spreadsheet-based data reduc-tion for laser ablation ICP–MS 315. In Sylvester P. (ad) Laser Ablation–ICP–MS in the Earth Sciences, Current Practices and outstanding issues, Appendix A4: Software for Reduction of LA–ICP–MS Data. MAC Short Course Series 40, 305-306.

Košler, J. & Sylvester, P. 2003. Present trends and the future of zircon in geochronology: la-ser ablation ICPMS. Reviews in Mineralogy & Geochemistry, 53, 243-275.

Ludwig, K.R. (2003) IsoplotEx v. 3.0. Berkeley Geochronological Center.

3.40

First insights into the dehydration of lizardite

Trittschack Roy & Grobéty Bernard

University of Fribourg, Department of Geosciences, Chemin du Musée 6, CH-1700 Fribourg (roy.trittschack@unifr.ch)

Lizardite $Mg_3Si_2O_5(OH)_4$ is a trioctahedral 1:1 phyllosilicate, which belongs together with chrysotile and antigorite to the serpentine mineral group. The structure of lizardite, based on simple flat lying T-O, is much simpler compared to the corrugated and cylindrical structures of antigorite and chrysotile respectively. Lizardite is, therefore, the logic starting point in an attempt to understand the dehydration processes and rates of this mineral group.

The aim of this study is to understand the rate determining steps and the kinetics of the dehydration of lizardite. The dehydration implies the deprotonation of part of the hydroxyl groups and recombination of the hydrogen ion with neighbouring hydroxyl groups to form a water molecule. The second step is the transport of the water molecule out to the surface. High-temperature experiments like in-situ HT-XRD and in-situ IR spectroscopy are ideally suited to investigate the structural changes during the reaction. Exploratory IR experiments and XRD studies on lizardite under room conditions gave starting temperatures for the dehydration between 500°C and 550°C which lies in the range of former investigations by Brindley & Zussman (1957) and Frank et al. (2005). The initial product of dehydration is amorphous, which crystallizes after a certain time

to forsterite followed by enstatite. Assuming proportionality between the integral intensity of hkl-peaks and the amount of lizardite present, the reaction rate can be extracted from the rate of intensity decrease. The data will be treated with the conventional Avrami method as well as the so called "time to a given fraction" (TGF) method. One major advantage of the TGF method is the possibility to discover changes in the activation energy E_a during the course of dehydration (Putnis, 1992). Known values for the activation energy of lizardite derived from differential thermal analyses (DTA) and lying around 350kJ mol^{-1} (Weber & Greer, 1965), which is rather large compared with other phyllosilicates with values around 200kJ mol^{-1}.

REFERENCES

Brindley, G.W. & Zussman, J. 1957: A structural study of the thermal transformation of serpentine minerals to forsterite. American Mineralogist, Vol. 42(7-8), 461-474.

Frank, M.R., Earnest, D.J., Candela, P.A., Wylie, A.G., Wilmot, M.S. & Maglio, S.J. 2005 (abstract): Experimental study of the thermal decomposition of lizardite up to 973K, Salt Lake City Annual Meeting 2005

Putnis, A. 1992: Introduction to Mineral Sciences, Campridge University Press, 457 p.

Weber, J.N. & Greer, R.T. 1965: Dehydration of serpentine - Heat of reaction and reaction kinetics at PH2O=1 Atm. American Mineralogist, Vol. 50(3-4), 450-464.

3.41

Analytical and numerical description of tephra deposition: the example of two large explosive eruptions of Cotopaxi Volcano, Ecuador

Tsunematsu Kae*, Bonadonna Costanza*, Falcone Jean-Luc** & Chopard Bastien**

*Département de Minéralogie, Université de Genève, Rue de Maraîchaire 13, CH-1205 Genève

** Département d'Informatique, Université de Genève, Battelle, Building A, Carouge; 7 route de Drize, CH-1227 Carouge

The downwind and crosswind tephra deposition was studied in detail for two large explosive eruptions of Cotopaxi volcano, Ecuador (a pumiceous unit, Layer 3, and a scoriaceous unit, Layer 5; Barberi et al. 1995). The two eruptions were characterized by a similar plume height, i.e. 28 ± 2 km for Layer 3 and 28 ±0 km for Layer 5, but Layer 3 was characterized by a larger volume, i.e. 1.5 km^3 for Layer 3 and 0.3 km^3 for Layer 5 (Biass and Bonadonna, submitted). The two layers are characterized by similar total grain size distribution (Md_Φ: ~-2), but Layer 3 tephra was advected by a stronger wind (28 m/s for Layer 3 and 21 m/s for Layer 5). As a result, crosswind variation of grain size is consistent for the two layers, but at any given distance from vent downwind deposition is coarser for Layer 3 (Figure 1). The increase rate of Md_Φ is about 0.2 for both layers (Figure 1a).

We have implemented both the model of Bonadonna and Phillips (2003) for tephra dispersal from strong volcanic plumes and the Cellular Automata model of Tsunematsu et al. (2008) to describe crosswind tephra deposition based on a Gaussian distribution. In addition, we have also implemented the model of Tsunematsu et al. (2008) to account for sedimentation from the bottom of the umbrella cloud as supposed to a point-source particle considering the following equation (Bonadonna and Phillips 2003):

$$M = M_0 \exp - \left\{ \int_{x_0}^{x} \frac{w}{Q} dx \right\} \quad (1)$$

where M (kg) is the total mass of particles of a given size fraction at the bottom of the spreading current, M_0 (kg) is the initial mass injected into the spreading current, Q is the volumetric flow rate, v is the terminal velocity of the particle of given grain size, w is the maximum crosswind width and x is the distance from the plume. Both the model of Bonadonna and Phillips (2003) and Tsunematsu et al. (2008) had shown good agreement with tephra deposition observed along the dispersal axis for a number of eruptions. However, the crosswind deposition had not been investigated in detail.

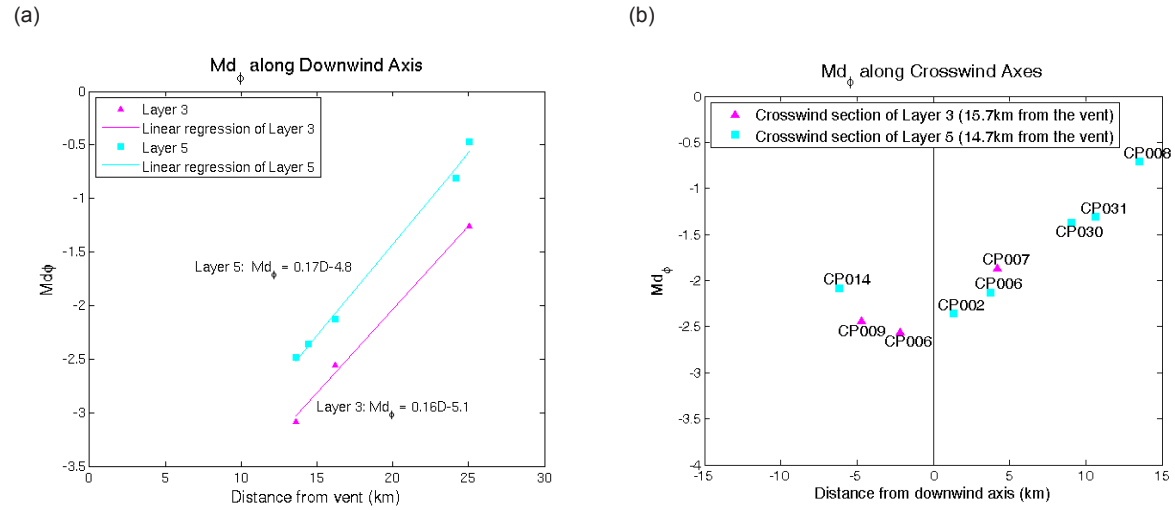

Figure 1. Median of grain size distribution along downwind axes (a) and crosswind axes (b). Pink triangles are data for Layer 3 and blue squares are data for Layer 5. For the downwind data, linear regressions are calculated for each layer. Pink line is for Layer 3 and blue line is for Layer 5.

REFERENCES

Barberi, F., Coltelli, M., Frullani, A., Rosi M., & Almeida, E. 1995: Chronology and dispersal characteristics of recently (last 5000 years) erupted tephra of Cotopaxi (Ecuador): implications for long-term eruptive forecasting. JVGR, 69, 217-239.

Biass S. & Bonadonna C., (in preparation) A quantitative uncertainty assessment of eruptive parameters derived from tephra deposits.

Bonadonna C. & Phillips J. C. 2003: Sedimentation from strong volcanic plumes. JGR. 108. B7, 2340, doi:10.1029/2002JB002034.

Tsunematsu K, Falcone JL, Bonadonna C & Chopard B. 2008: Applying a Cellular Automata Method for the Study of Transport and Deposition of Volcanic Particles H. Lecture Notes in Computer Science (LNCS). vol. 5191, 393-400.

3.42

Petrology of mafic-ultramafic complexes within the Archean Lewisian complex of NW Scotland

Udry Arya*, Müntener Othmar*,

* *Institute of Mineralogy and Geochemistry, University of Lausanne, Anthropole, CH-1015 Lausanne (arya.udry@unil.ch)*

The Lewisian complex is a fragment of the ancient Laurentian continental mass, the southern extension, which is now buried beneath the metasediments of the Scottish highlands. The Archean gneisses of the Lewisian complex represent a long, and complex part of Earth history.

The area of interest is in Northwestern Scotland, between Loch Laxford and Loch Inver. The terrain consists mostly of banded gneisses with a variety of basic to ultrabasic bodies. The gneisses are banded with alternating acid and mafic layers. Granulite facies parageneses are common. Large bodies of ultrabasic rocks contain variable proportions of olivine, pyroxene, spinel, plagioclase and hornblende, whereas basic bodies are essentially made of pyroxene, hornblende, plagioclase and garnet bearing assemblages. This study focuses on two of these complexes near Drumbeg and near Scourie. These bodies are described as layered 'meta' intrusives and are embedded within tonalitic to granodioritic gneisses.

Isotopic studies indicate that the gneisses derived from magmas that separated from the mantle about 2.9 Ga (Moorbath and al. 1969; Hamilton and al. 1979) and the high grade metamorphism was completed by about 2.7 Ga (Chapman and Moorbath 1977). Later dikes (Scourie dikes) are dated at 2.4 Ga (Chapman 1979), followed by retrograde amphibolite facies metamorphism and injection of granites and pegmatites at about 1.8 Ga. (Johnstone and Mykura 1989).

Several hypotheses have been put forward about the formation of those ultramafic and mafic bodies, but it has been demonstrated that voluminous granodiorite and tonalite surrounding rocks are of calc-alkaline affinity, which is generally inferred to be important in subduction zone environments. After Park and Tarney (1987), gneisses represents continental crust formed during subduction and the mafic-ultramafic association represents material intercalated tectonically during processes of crustal generation, probably from subducting ocean floor. This interpretation might be debated. We evaluate the hypothesis whether such rock associations could be related to crystallization from H_2O-rich magmas within an Archean

subduction zone environment, or alternatively, whether they could be related to metamorphosed dry plutonic rocks within the Archean crust, by applying new mapping and systematically investigating mineral chemical major and trace element data.
It is entirely unknown, whether primary igneous phases are still present (e.g. Sills et al. 1982) and apparent granulite facies "metamorphic" textures mask the igneous crystallisation history of this high pressure rocks. However, with the application of new in-situ methods such as Laser Ablation ICP-MS, new results on the main minerals and whole rocks were obtained. In addition, we will determine in-situ the major and trace element distribution of the major mineral phases that should provide additional constraints on the equilibration history of these rocks. We focus on elements distributions and garnets zonations and try to evaluate a magmatic vs metamorphic origin.
We present preliminary results on the thermal evolution of mafic-ultramafic systems within granulite facies host rocks. Testing the hypothesis of an arc origin is not only an important question for a better understanding of the Archean Lewisian complex, but much more so for the importance how subduction processes worked in the Archean.

REFERENCES

Chapman, H.J. (1979): 2390 M.yr Rb-Sr whole rock isochron for the Scourie dykes of NW Scotland. Nature, 277, 642

Chapman H.J., Moorbath S. (1977): Lead isotope measurements from the oldest recognized Lewisian gneisses of north-west Scotland. Nature, 268, 41-42

Hamilton P.J., Evensen N.M., O'Nions R.K., Tarney J. (1979): Sm-Nd systematics of Lewisian gneisses : implications for the origin of granulites. Nature, 277, 25-28

Johnstone, G.S. and Mykura, W. (1989): British regional geology: the northern Highlands of Scotland (4th edition). British Geological Survey, pp219

Moorbath S., Welke H., Gale N.H. (1969): The significance of lead isotope studies in ancient, high grade metamorphic basement complexes, as exemplified by the Lewisian rocks of Northwest Scotland. Earth Planet Sci Lett, 6, 245-256

Park, R.G. and Tarney, J. (1987): The Lewisian complex : a typical Precambrian high-grade terrain? Evolution of the Lewisian and comparable Precambrian high grade terrains, Geological Society Publication, 27, 13-25

Sills, J.D., Savage, D., Watson, J.V., and Windley, B.F. (1982): Layered ultramafic-gabbro bodies in the Lewisian of northwest Scotland: geochemistry and petrogenesis. Earth and Planetary Science Letters, 58, 345-360

3.43

Iridium-strip heater glass pellets: Effects of fusion temperature and time on Li, Be and B content

Vils Flurin*, Dijkstra Arjan*, Laure Pelletier*, Thomas Ludwig** & Angelika Kalt*

*Institut de Géologie et d'Hyrogéologie, Rue Emile-Argand 11, Cp158, 2009-Neuchâtel (flurin.vils@unine.ch)
**Institut für Geowissenschaften, Im Neuenheimer Feld 236, D-69120 Heidelberg

To solve a broad range of geochemical problems, precise and accurate whole rock and trace element analyses are required. Especially in the case of low abundant elements like Li, Be and B, which are widely used as tracers of alteration, subduction and recycling processes in the Earth, this is a critical issue. For in-situ mineral measurements of these elements, secondary ion mass spectrometry (SIMS) is probably the most sensitive and most accurate. A method that allows to analyse whole rock light element concentrations using SIMS would be extremely powerful and would dramatically increase sample throughput. However, a method to measure whole rock contents of all three light elements together is missing so far.
An Iridium-strip heater provides a flux free method to fuse directly homogeneous glass pellets from powdered rocks. These pellets can be investigated for major and light elements using microbeam (electron, ion or laser) methods. We have conducted experiments under different fusion temperatures (1500-1800°C) and time (30-240 s) on selected samples representing a wide variety of Li (0.91 to 56.5 μg/g), Be (0.24 to 3.5 μg/g) and B content (2.18 to 12 μg/g). We studied the behaviour of the three elements with respect to the different compositions, fusion time and temperature.
Homogeneity within the fused glasses is generally reached under the studied conditions for most elements. Electron microprobe measures and element distribution maps confirm this homogeneity. Light element measurements showed homogeneous behaviour for Li and Be (RSD of 3%, 6% respectively), but B is significantly less homogeneous (average RSD of 31%). Heating time dependent loss of Li, Be and B occurs throughout all studied samples, but Be and Li loss is always within analytical errors of the used methods (generally <10%). Significant B loss during fusion is found in almost every sample. In general, B is showing highly volatile behaviour, and at 1800°C most B has evaporated. Clearly, flux-less preparation of whole rock glasses is not a viable method for B analysis because of its volatility, but the method is well-suited for Li and Be.

3.44

Molybdenum isotopes in modern corals: investigation into their potential as redox proxy of bygone oceans

Voegelin, Andrea R.*, Samankassou, Elias* & Nägler, Thomas F.**

* *Département de Géologie et Paléontologie, Université de Genève, Rue des Maraîchaire 13, CH-1205 Genève (andrea.voegelin@unige.ch)*
** Institut für Geologie, Universität Bern, Baltzerstrasse 1+3, CH-3012 Bern

Periods of marine O_2 deficiency are important features of Earth history, in particular for climate and the evolution of life. The oxygenation state of paleo-environments is closely connected to the cycling of redox sensitive elements. Hence, the interpretation of past changes in oceanic redox chemistry depends on the identification of geochemical proxies which provide a reliable fingerprint of past seawater compositions.

In recent years the molybdenum isotope system has attracted significant attention and has proven to be useful in the investigation of the extent of sea-floor anoxia in the geological past (e.g. Arnold et al., 2004, Wille et al., 2008, Pearce et al., 2008). Carbonate rocks have just recently been introduced as promising new Mo isotope archive (Voegelin et al., 2009). It was shown that Mo uptake into non-skeletal carbonate precipitates is accompanied by minor isotope fractionation. Consequently, they were proposed as a monitor of the ambient fluid composition, which, under favorable conditions, may closely reflect the ocean water $\delta^{98/95}$Mo of bygone oceans. The application of skeletal carbonate is complicated by biologically controlled isotope fractionation, which may completely obliterate the original ocean water signature (Voegelin, 2009). So far, only well preserved modern aragonitic corals have revealed to exhibit a consistently small offset from seawater. They may thus provide the means to obtain a well dated and nearly continuous reconstruction of the Mo isotopic composition of past oceans from the Holocene as far back as Ordovician times. Their application as paleo-oceanographic tool, however, depends on the preservation of an ocean water signature during diagenetic processes, especially the replacement of meta-stable skeletal aragonite with calcite.

This study investigates unaltered coral matrices and diagenetically modified material in order to assess possible post-depositional Mo isotope and trace element exchange processes and their implications for the future use of corals as Mo archive.

REFERENCES

Arnold, G. L., Anbar, A. D., Barling, J. & Lyons, T. W, 2004: Molybdenum isotope evidence for widespread anoxia in mid-Proterozoic oceans. Science, 304, 87-90.

Pearce, C. R., Cohen, A. S., Coe, A. L. & Burton, K. W., 2008: Molybdenum isotope evidence for global ocean anoxia coupled with perturbations to the carbon cycle during the early Jurassic. Geology, 26 (3), 231-234.

Voegelin, A. R., Nägler, T. F., Samankassou, E. & Villa, I. M., 2009: Molybdenum isotopic composition of modern and Carboniferous carbonates. Chemical Geology, 265, 488-498.

Wille, M., Nägler, T. F., Lehmann, B., Schröder, S. & Kramers, J. D., 2008: Hydrogen suphide release to surface waters t the Precambrian/Cambrian boundary. Nature, 453, 767-7.

3.45

Effect of minor elements (H^+ and Al^{3+}) on the elastic properties of orthopyroxenes

Jingyun Wang*, Carmen Sanchez-Valle* & Roland Stalder**

* *ETH, Inst Mineral & Petrol, CH-8092 Zurich (jingyun.wang@erdw.ethz.ch)*
** *Innsbruck Univ, Inst Mineral & Petrog, A-6020 Innsbruck, Austria*

Orthopyroxenes (Opx), along with olivine, garnets and clinopyroxenes, are major components of the upper mantle. Knowledge of the changes in seismic velocities and elastic properties of Opx as a function of composition is therefore essential to build up mineralogical models of the upper mantle and to interpret heterogeneities in the mantle revealed by high-

resolution seismic tomographic images. While the elastic properties of Mg- and Fe-end-members have received much attention over the past years, the influence of minor element substitutions on the elastic properties of orthopyroxenes has been less investigated.

Here we present Brillouin scattering measurements of the single-crystal elastic properties of synthetic hydrous aluminum-free and hydrous aluminum-bearing orthopyroxenes (hereafter referred to as HyOpx and AlOpx, respectively) under ambient conditions. The samples were synthesized at 2.5 GPa and 1150 °C in piston-cylinder apparatus. HyOpx contains minor amounts of H^+ (280 ppm H_2O) while AlOpx has a similar Al_2O_3 content (6.3 wt%) to that of natural Opx, and minor amounts of H^+ (1500 ppm H_2O), and Fe (0.26wt% FeO). The aggregate bulk (K_S) and shear (μ) elastic moduli of HyOpx, K_S = 108.5(9) GPa and μ = 77.0(4) GPa, are indistinguishable from those of anhydrous orthoenstatite. The results suggest that incorporation of H_2O up to 280 ppm has no significant influence on elastic properties of $MgSiO_3$-orthoenstatite. The aggregate elastic moduli of AlOpx, K_S = 126.2(1.2) GPa and μ = 81.3(8) GPa, are respectively 14.7 and 6% higher than those of pure $MgSiO_3$-orthoenstatite. These results confirm that the stiffening of the bulk modulus reported in natural Opx relative to Mg-end-members is mainly due to the substitution of Al for smaller Si in tetrahedral sites. This conclusion is supported by the strong increase in the C_{33} elastic constant upon Al substitution that reflects the stiffening of the tetrahedral chains running along c-axis. Consequently, the aggregate velocities of AlOpx, V_P = 8.50(9) km/s and V_S = 5.01(6) km/s, are 7% and 4% higher than those of the magnesian end-member. The results indicate that Al has the strongest effect on the seismic velocities of Opx of all minor elements and may be taken into account to refine compositional and mineralogical models of the upper mantle.

3.46

Deciphering the Alpine orogenic and thermal evolution from subduction to collision: Raman spectroscopy and 40Ar/39Ar age constraints from the Valaisan Ocean (Central Alps)

Wiederkehr Michael*, Bousquet Romain**, Sudo Masafumi**, Ziemann Martin A.**, Berger Alfons*** & Schmid Stefan M.****

*Bundesamt für Landestopografie swisstopo, Landesgeologie, Seftigenstrasse 264, CH-3084 Wabern, Switzerland (michael.wiederkehr@swisstopo.ch)
**Institut für Geowissenschaften, Universität Potsdam, Karl-Liebknecht-Strasse 24/25, D-14476 Potsdam/Golm, Germany
***Institut for Geografi og Geologi, Københavns Universitet, Øster Voldgade 10, DK-1350 København K, Denmark
****Institut für Geologische Wissenschaften, Freie Universität, Malteserstrasse 74-100, D-12249 Berlin, Germany

The metasediments of the Valaisan Ocean and the adjacent distal European margin, exposed between the Pizzo Molare/Passo di Lucomagno area and the Prättigau half-window show a remarkable metamorphic gradient: Carpholite bearing assemblages in the east indicate pressure dominated blueschist facies metamorphism. Further west the same units are characterized by a temperature dominated Barrovian amphibolite facies metamorphism ("Lepontine" metamorphism). The relationships between deformation and metamorphism indicate two distinct metamorphic events: a late-stage Barrowian ("Lepontine") event clearly overprints an earlier HP/LT event. This is independently confirmed by a bimodal P-T path (Wiederkehr et al., 2008). To unravel this poly-metamorphic evolution we performed detailed investigations of carbonaceous matter by Raman spectroscopy in order to monitor the spatial distribution of peak-metamorphic temperatures. Additionally, we performed $^{40}Ar/^{39}Ar$ dating of mica by using in-situ and step-wise-heating techniques in order to decipher the temporal relationships between these two metamorphic events. The new data yield important insight regarding the transition from subduction to collision, both on the scale of the tectonic units derived from the Valaisan paleogeographical domain and on the scale of the entire orogenic belt.

The results of Raman spectroscopy, performed on a total of 214 samples, allow for high resolution mapping of the maximum metamorphic temperatures reached in these samples in three dimensions. Such three-dimensional mapping of the isotemperature contours in map and profile view faithfully reflects the present-day distribution of peak-metamorphic temperatures. The temperature gradients resulted from a superposition of at least three distinct metamorphic events (Wiederkehr et al., submitted). (1) Within the northeastern rim of the Lepontine dome - both along and across strike - the isotemperature contours in the 450-570 °C temperature interval are associated with the collision-related late-stage Barrow-type event. They clearly cut across nappe contacts and mega-folds deforming such older tectonic contacts. (2) Further to the NE the 350-425 °C isotemperature contours reflect temperatures reached during an earlier blueschist facies event and/or subsequent near-isothermal decompression. They are folded by large-scale post-nappe stacking mega-folds. (3) A substantial "temperature jump" across the tectonic contact between the frontal Adula nappe complex (500-520 °C) and the surrounding Valaisan-de-

rived metasediments (410-430 °C) indicates that, in contrast to the postulates raised by earlier studies, equilibration of temperatures during the late-stage Lepontine event is incomplete in this area.

The dating of high-pressure metamorphism, subsequent retrogression and final Barrow-type overprint was obtained by $^{40}Ar/^{39}Ar$ dating of biotite and different white mica generations that are all well characterized in terms of mineral chemistry, texture and associated mineral assemblages (Wiederkehr et al., in press). Four distinct age populations of white mica record peak-pressure conditions at 42-40 Ma, followed by several stages of a retrograde metamorphic evolution, predominantly decompression, between 36 and 25 Ma. Biotite isotopic analyses yield consistent apparent ages that cluster around 18-16 Ma for the Barrow-type thermal overprint that was associated with the temperature increase that followed decompression. The isotopic data reveal a significant time gap in the order of some 20 Ma between the subduction-related HP/LT event (42-40 Ma) and the later collision-related MP/MT Barrovian overprint (19-18 Ma). This substantial time gap, together with the age constraints on white mica reflecting the retrograde metamorphic evolution of the HP/LT stage, support the notion of a poly-metamorphic evolution associated with a bimodal P-T path. Amphibolite facies Barrow-type overprint of the NE Lepontine dome clearly represents a separate heating pulse that post-dates isothermal decompression after the high-pressure stage. This indicates that it is the accretion of vast amounts of European continental crust forming the present-day Lepontine dome that provides high radiogenic heat production responsible for amphibolite facies metamorphism (Bousquet et al., 2008]. This heating is an entirely conductive and therefore rather slow process.

REFERENCES

Bousquet, R., Oberhänsli, R., Goffé, B., Wiederkehr, M., Koller, F., Schmid, S.M., Schuster, R., Engi, M., Berger, A. & Martinotti, G. 2008: Metamorphism of metasediments at the scale of an orogen: A key to the Tertiary geodynamic evolution of the Alps. In: S. Siegesmund et al. (eds.) Tectonic Aspects of the Alpine-Dinaride-Carpathian system, Geol. Soc. Special Publ., 298, 393-411.

Wiederkehr, M., Bousquet, R., Schmid, S.M. & Berger, A. 2008: From subduction to collision: Thermal overprint of HP/LT meta-sediments in the north-eastern Lepontine Dome (Swiss Alps) and consequences regarding the tectono-metamorphic evolution of the Alpine orogenic wedge. In: N. Froitzheim & S.M. Schmid (eds.) Orogenic processes in the Alpine collision zone, Swiss J. Geosci., 101(Suppl), S127-S155.

Wiederkehr, M., Sudo, M., Bousquet, R., Berger, A. & Schmid, S.M. in press: Alpine orogenic evolution from subduction to collisional thermal overprint: 40Ar/39Ar age constraints from the Valaisan Ocean (Central Alps), Tectonics.

Wiederkehr, M., Bousquet, R., Ziemann M.A., Berger, A. & Schmid, S.M. submitted: 3-D assessment of peak-metamorphic conditions by Raman spectroscopy of carbonaceous material: an example from the margin of the Lepontine dome (Swiss Central Alps), submitted to Contrib. Mineral. Petrol.

3.47

Approximate terrestrial age dating of meteorites by use of handheld XRF

Zurfluh Florian*, Hofmann Beda**, Gnos Edwin***, Eggenberger Urs* & Opitz Christoph**

*Institut für Geologie, Baltzerstrasse 1+3, CH-3012 Bern (florian.zurfluh@geo.unibe.ch)
**Naturhistorisches Museum Bern, Bernastrasse 15, CH-3005 Bern
***Muséum d'Histoire naturelle, route de Malagnou 1, CP 6434, CH-1211 Genève

During a large project for systematic meteorite search in the hot desert of the Sultanate of Oman we have so far collected 5237 samples that represent ~550 fall events. This is, besides the Antarctic collection, the largest well-characterised meteorite population. Our main goals are to evaluate statistically our finds and study the weathering and contamination effects of the samples during their terrestrial residence. For these purposes we need to know how long the meteorites are on earth. Usually the terrestrial age is determined by ^{14}C measurements (e.g. Jull 2006). But these analyses are time consuming and there is no chance to measure all collected samples. Former studies have shown a continuous uptake of Sr and Ba during the terrestrial sojourn of meteorites (e.g. Al-Kathiri et al. 2005). We try to calibrate an age scale for fast dating of Omani meteorites by use of Sr contents measured with handheld XRF.

We use a Niton XL3t-600 handheld XRF analyser for fast and non-destructive measurements of nearly all elements between K and U, with a special focus on Fe, Mn, Ni, Ca and the weathering proxy Sr. This instrument has a predefined measurement mode for trace elements in medium concentrations. Tests with international and own meteorite standards measured with ICP-MS and handheld XRF confirmed an accuracy of Sr measurements with this "soil mode" within a derivation of ± 13 % at counting times of 120 seconds. Initial Sr contents in ordinary chondrites, the most abundant group of meteorites, are between 10 and 11.1 ppm (Wasson & Kallemeyn 1988) whereas they can reach values of several thousand ppm during weathering and contamination.
Another effect might be useful for relative dating: in hot deserts occurs an accumulation of Mn-rich material during exposure time on some rocks. It is also possible to quantify this desert varnish with handheld XRF.

Measurements were performed on cut- (C), exposed- (E) and buried-surfaces (V) of meteorites from five large strewn fields and some individual samples collected on two major meteorite recovery surfaces in the Sultanate of Oman, the Dhofar (Dho)/ Shisr region and Jiddat al Harasis (JaH)/Sayh al Uhaymir (SaU). The influence of the soil is evident but a lot of analysis of Omani desert soil samples delivered low variations for Sr concentrations somewhere between 250 to 350 ppm (Al-Kathiri et al. 2005). From each strewn field seven to 25 samples were analysed on the three mentioned surfaces (C,E and V). Each surface was measured for at least three times to minimise effects of local inhomogeneities.

The results of this survey were compared with ^{14}C ages from Al-Kathiri et al. (2005). The samples from the youngest strewn field, SaU001, have in general the lowest Sr contents. As one would expect the highest values are measured on the outer surfaces (V) of the samples that were buried in the soil, approve the contamination of the meteorites with Sr from the soil. The young and medium age samples (SaU001, JaH073 & JaH091) have high differences between the outer (E, V) and the interior (C) Sr concentrations whereas the older samples (Shisr015 & Dho005) have a more balanced ratio between the surfaces. A continuous diffusion of Sr from the exterior to the interior is a plausible explanation for this effect.
The cut surfaces deliver the best values for an approximate age dating. There is an inconsistency between the Sr contents at the cut surface and the ^{14}C age of the two JaH strewn fields. Since these are extremely large strewn fields, shielding effects could have falsified the radiocarbon age (Gnos et al. 2006, 2009). The younger "Sr age" of the JaH091 is supported by a general lower degree of weathering observed in thin section. Additionally the JaH073 samples have a more elevated Mn enrichment on the exposed surfaces that indicates a thicker desert varnish and therefore longer residence time in the desert.

With a combined study of the weathering grade observed in thin section, fast measurement by handheld XRF of Sr on cut surfaces and the degree of Mn enrichment on exposed surfaces it should be possible to estimate approximate the terrestrial ages of Omani meteorites.

REFERENCES

Al-Kathiri, A., Hofmann B. A., Jull A. J. T., and Gnos E. 2005: Weathering of meteorites from Oman: Correlation of chemical/ mineralogical weathering proxies with 14C terrestrial ages and the influence of soil chemistry, Meteoritics & Planetary Science, 40, 1215-1239.

Gnos, E., Eggimann M. R., Al-Kathiri A. and Hofmann B. A. 2006: The JaH091 strewn field, Meteoritics & Planetary Science 41 Suppl., A64

Gnos, E., Lorenzetti S. R., Eugster O., Jull A. J. T., Hofmann B. A., Al-Kathiri A and Eggimann M. R. 2009: The Jiddat al Harasis 073 strewn field, Sultanate of Oman, Meteoritics & Planetary Science 44, Nr 3, 375-387

Jull, T. 2006: Terrestrial Ages of Meteorites. In Meteorites and the Early Solar System II (eds. D. S. Lauretta and H. Y. McSween), pp. 889-905. University of Arizona Press, Tucson.

Wasson, J.T. & Kallemeyn G.W. 1988: Compositions of chondrites, Phil.Trans.R.Soc.Lond. A325, 535-544